Chromosoma (2025) 134:10
https://doi.org/10.1007/s00412-025-00839-z

RESEARCH

The synaptonemal complex component corolla regulates meiotic crossover formation in *Drosophila melanogaster*

Stefanie Williams[1] · Grace McKown[1] · Zulin Yu[1] · Jennifer Gardner[1] · Cynthia Staber[1] · Matthew C. Gibson[1] · R. Scott Hawley[1]

Received: 23 June 2025 / Revised: 15 October 2025 / Accepted: 28 October 2025 / Published online: 10 November 2025
© The Author(s) 2025

Abstract

In *Drosophila melanogaster* females, as in most organisms, the segregation of homologous chromosomes in meiosis depends on the formation of crossovers between them. In most cases, crossovers require the synaptonemal complex (SC), a conserved multi-protein structure that forms between homologous chromosomes in early meiosis. Recent studies leveraging partial-loss-of-function alleles suggest that the SC plays a more direct role in crossover formation. One SC protein that is involved in crossover formation is SYP-4 in nematodes, which we found is a likely ortholog of the *D. melanogaster* SC protein Corolla. To create a hypomorphic allele of *corolla* in *D. melanogaster*, we used CRISPR/Cas9 to replace it with its *D. mauritiana* ortholog, yielding *corolla*^{mau}. Since SC protein sequences are rapidly diverging while maintaining the SC's structure, we hypothesized that this replacement would enable SC assembly but show defects in crossover formation. Indeed, at 25 °C *corolla*^{mau} homozygous females exhibited defects in SC maintenance and crossover formation, resulting in moderate levels of chromosome missegregation. At 18 °C, SC maintenance was rescued, and recombination rates were improved, although they remained significantly lower than observed in wild type. Unexpectedly, in homozygotes we also observed unique polycomplexes composed of the SC proteins Corolla and Corona but lacking the transverse filament protein C(3)G. Overall, we report a novel hypomorphic allele of *corolla* that suggests Corolla regulates crossover formation. Further, the unique polycomplexes found in mutant flies may provide new insights into SC architecture and protein-protein interactions.

Keywords Meiosis · Synaptonemal complex · Recombination · Hypomorph · Crossover

Introduction

Sexual reproduction relies heavily on the successful completion of meiosis. This specialized form of cell division reduces the chromosome number by half, ensuring that when an egg and sperm fuse, the correct ploidy is achieved. Mistakes during meiosis can lead to the improper segregation of chromosomes resulting in aneuploidy which is the leading cause of miscarriages and congenital syndromes such as trisomy 21 (Hassold et al. 2007; Llano and Pendás 2023; Adams and Davies 2023).

In most organisms, the formation of meiotic crossovers between homologous chromosomes is essential to ensure their proper segregation (Koehler et al. 1996). These crossovers mature into chiasmata which hold the homologs together until they can be separated in anaphase I. Importantly, crossovers are not randomly distributed across the chromosomes. Instead, several mechanisms ensure their proper positioning (reviewed in (Pazhayam et al. 2021). Crossover assurance ensures that a minimum of one crossover is established between each homologous chromosome pair (reviewed in (Wang et al. 2015b). In most species, the centromere effect suppresses the formation of crossovers within the centromere as well as the euchromatin in proximity to it. Precisely how proximal to the centromere a crossover can form differs between organisms (Pazhayam

R. Scott Hawley is deceased. This paper is dedicated to his memory.

✉ Stefanie Williams
swilliams@stowers.edu

✉ Matthew C. Gibson
mg2@stowers.org

[1] Stowers Institute for Medical Research, Kansas City, MO, United States of America

et al. 2021, 2025; Sen et al. 2023; Fernandes et al. 2024). Similarly, crossovers are suppressed within and close to the telomeres, the ends of chromosomes generally consisting of repetitive non-coding DNA sequences and heterochromatin in most organisms (Zakian 2012; Pazhayam et al. 2021). In addition, crossover interference enforces that two crossovers cannot occur in close proximity to one another, although the strength of this effect varies dramatically between species (Pazhayam et al. 2021; Sen et al. 2023; Girard et al. 2023). The lengths of chromosome axes also play into the patterning of crossovers (Pazhayam et al. 2021). As a result, crossover patterning is species-specific with observable differences even between closely related species. This is seen in *Drosophila melanogaster* and its close relatives *Drosophila mauritiana* and *Drosophila simulans*, both of which present with a larger map length and more centromere-proximal crossovers compared to *D. melanogaster* (True et al. 1996; Hawley et al. 2025).

The precise role of the synaptonemal complex (SC) in the regulation of crossover formation and distribution remains poorly understood. The SC is a multi-protein structure that consists of two lateral elements connected to the homologous chromosomes and the central region with a central element that synapses them (Fig. 1a). The protein components that make up the SC differ among established meiosis research organisms. To our current knowledge, the central region of the SC in *D. melanogaster* is comprised of three proteins: C(3)G, Corolla, and Corona (Cona) (Fig. 1a) (Page and Hawley 2001; Page et al. 2008; Collins et al. 2014). C(3)G is the transverse filament protein (Page and Hawley 2001). The C-termini of C(3)G are thought to interact with both lateral elements while the N-termini are thought to interact with the N-termini of another C(3)G dimer (Page and Hawley 2001; Anderson et al. 2005; Cahoon et al. 2017). The localization of Corolla within the SC has been described as transverse filament-like (Collins et al. 2014; Cahoon et al. 2017). Immunofluorescent labeling in combination with expansion microscopy and structured illumination imaging revealed that Corolla does not span the entire width of the SC from one lateral element to the other, but the signal is too wide for it to be considered a central element protein (Cahoon et al. 2017). Cona is known as the central element protein of *D. melanogaster* with a distinct localization in the very center of the SC (Page et al. 2008; Cahoon et al. 2017).

In most organisms, the fully assembled synaptonemal complex (SC) is required for meiotic crossover formation and thus accurate chromosome segregation. However, several exceptions have been found. In *Saccharomyces cerevisiae*, mutants missing the central element components Ecm11, Gcm2, or the majority of the transverse filament protein Zip1 N-terminus have higher levels of recombination despite lacking full-length SC (Voelkel-Meiman et al. 2016). In *Arabidopsis thaliana*, double *null mutants* of the transverse filament proteins *zyp1a* and *zyp1b* resulted in asynapsis while crossover formation remained possible (Capilla-Pérez et al. 2021; France et al. 2021). The proper regulation of these crossovers was disrupted, resulting in the loss of crossover assurance for each chromosome, loss of crossover interference, and loss of typically observed sex

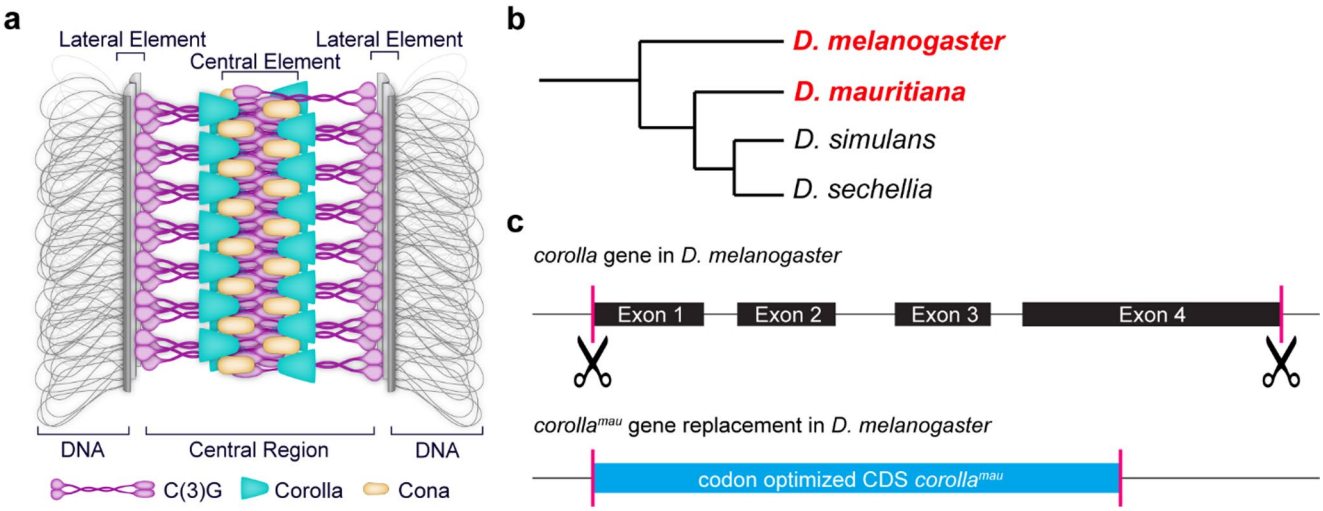


Fig. 1 The replacement of the SC central region protein Corolla with its ortholog from *D. mauritiana*. (**a**) Model of the SC in *D. melanogaster*. The lateral element is connected to chromatin of the homologous chromosomes. Within the central region of *D. melanogaster* is the transverse filament protein C(3)G, Corolla, and the central element protein Cona. (**b**) The cladogram shows the closest relatives to *D. melanogaster* that are *D. mauritiana*, *D. simulans*, and *D. sechellia.* For the gene replacement of *corolla*, we chose *D. mauritiana*. (**c**) Schematic of how the gene replacement was performed. The gene *corolla* was excised from the start of exon 1 to the end of exon 4 using CRISPR/Cas9 technology. The codon optimized coding sequence (CDS) from *D. mauritiana* was then inserted in this same locus

differences in crossover rates (Capilla-Pérez et al. 2021; France et al. 2021). In *Oryza sativa*, the *zep1-3* mutant (expressing a truncated version of the transverse filament protein) shows elevated recombination rates and changes in crossover distribution (Wang et al. 2015a). While these findings show that synapsis of the homologs is not a requirement for crossovers in some species, the observed changes in crossover numbers and their distribution do suggest a role of the SC in crossover patterning.

Interestingly, while the basic architecture of the SC is conserved across eukaryotes, the protein components that make up the SC are rapidly evolving (reviewed in (Williams and Hawley 2025). This rapid evolution of SC components presents a significant challenge in studying the role the SC plays in crossover formation as it makes the identification of conserved amino acids difficult. Conserved residues within a protein's amino acid sequence are generally assumed to serve important functions, making them appropriate targets for mutagenesis (Billmyre et al. 2023). The rapid evolution suggests that changes to single amino acids can be tolerated without causing major meiotic defects and therefore do not cause easily recognizable phenotypes which can be recovered in genetic screens. A suppressor screen performed by Kursel et al. highlights this, as many of the recovered suppressors of the s*yp-1*^{K42E} mutant phenotype had acquired mutations in *syp-1* and *syp-3*, but displayed no additional phenotypes (Kursel et al. 2023). This indicates that many point mutations within SC genes are tolerated. As a result, most SC mutants recovered so far have been null alleles. While these mutants have been instrumental in understanding the essential role of the SC in crossover formation and chromosome segregation, the reliance on loss-of-function mutations comes with significant limitations. In most organisms, null alleles typically result in a complete failure of SC assembly, leading to an almost complete lack of crossover events between homologous chromosomes. This makes it challenging to genetically dissect the SC's role in regulating the formation and distribution of crossover events.

Despite these challenges, there are key examples of partial loss-of-function alleles that have permitted the study of the SC's role in recombination. In one case, targeted deletions in the *D. melanogaster* SC protein C(3)G suggested that the autosomes and the *X* chromosome require full-length SC at different times for their proper recombination (Billmyre et al. 2019). In *C. elegans*, lowering the expression levels of the transverse filament protein SYP-1 by RNAi resulted in a decrease of crossover interference (Libuda et al. 2013). Additionally, two recent studies showed that mutations in the *C. elegans* SYP-4 C-terminus disrupt normal crossover patterning (Köhler et al. 2025; Neves et al. 2025).

We found that the *D. melanogaster* SC protein Corolla is likely an ortholog of SYP-4 in *C. elegans.* In an effort to create a novel hypomorphic allele by leveraging the rapid evolution of SC proteins, we used CRISPR/Cas9 to replace *D. melanogaster corolla* with the ortholog from its close relative *D. mauritiana*. The two *Drosophila* species differ in their crossover landscape (True et al. 1996; Hawley et al. 2025), and their respective Corolla proteins share 86.7% amino acid sequence identity. We hypothesized that the replacement allele, referred to as *corolla*^{mau}, would result in a partial loss-of-function allele, as amino acid substitutions are found throughout the protein sequence. Indeed, we found that *corolla*^{mau} females exhibit temperature-sensitive synapsis defects and global crossover defects. At a rearing temperature of 25 °C, *corolla*^{mau} homozygous females assembled SCs in early pachytene but showed early fragmentation and early disassembly. In addition, *corolla*^{mau} mutants exhibited unusual polycomplexes (PCs) that contained Corolla and Cona but lacked the transverse filament protein C(3)G. These PCs suggest that the interaction of Corolla from *D. mauritiana* with Cona from *D. melanogaster* is functional but the interaction with C(3)G may be disrupted. We also observed significantly reduced levels of recombination on the *X* chromosome and, while not as severely affected, improper recombination levels and distribution of crossovers on the *2nd* chromosome. At 18 °C, SC maintenance was not negatively affected, correlating with an improvement of *X* chromosome recombination, although the levels were still significantly lower than in wild type (=*corolla*$^{+}$). As recombination overall was decreased but not abolished, chromosome missegregation was significantly increased but lower than observed for the *corolla*^{null} mutant. From this we infer that *corolla*^{mau} is a hypomorphic allele as homozygotes present with proper SC assembly and maintenance at 18 °C, but crossovers and chromosome segregation are significantly impacted. Together, these results suggest that by replacing the Corolla protein from *D. melanogaster* with its *D. mauritiana* ortholog we successfully altered proper crossover formation. In addition, these data support the hypothesis that Corolla is not only a structural protein of the SC but plays an additional role in crossover formation.

Materials and methods

Stock maintenance

All flies used here were maintained on standard food. Flies for the experiments at 25 °C–18 °C were reared at their respective temperature.

Construction of CRISPR stock

w^{1118}*hyb5b-8*, *corolla*^{mauEx1} was made by WellGenetics Inc. using a modified method of CRISPR/Cas9-mediated genome editing published by Kondo and Uedo in 2013 (Kondo and Ueda 2013). The upstream CRISPR/Cas9 target site was selected to be + 18 nt away from the start codon of *corolla* in *D. melanogaster* (CCCATAAATTCTTTGACAA G[TGG] with the PAM site in square brackets). The resulting upstream guide RNA primer oligos were the following: Sense oligo5'-CTTCGCCCATAAATTCTTTGACAAG and Antisense oligo 5'-AAACCTTGTCAAAGAATTTATGGG C. The upstream homology arm consisted of 1000 bp, specifically those − 1000 nt to −1nt upstream of the *corolla* start codon in *D. melanogaster*. The downstream CRISPR/Cas9 target was selected to be −21 nt away from the stop codon of *corolla* in *D. melanogaster* (ATGTACGCCGAGGCGG CAGT[AGG] with the PAM site in square brackets). The resulting downstream guide RNA primer oligos were the following: Sense oligo5'-CTTCGATGTACGCCGAGGCG GCAGT and Antisense oligo5'-AAACACTGCCGCCTCG GCGTACATC. The downstream homology arm consisted of 993 bp, specifically those + 4 nt to + 996 nt downstream of the stop codon of *corolla* in *D. melanogaster*. The knock-in cassette consisted of the codon optimized coding sequence of *corolla* in *D. mauritiana* and a selection marker to facilitate screening. The selection marker consisted of Piggy Bac 5' terminal repeats, the artificial 3xP3 promoter, DsRed2, SV40 3'UTR and Piggy Bac 3' terminal repeats. For codon optimization of the *corolla* CDS the IDT DNA codon optimization tool ((https://www.idtdna.com/CodonOpt) with the gBlocks option was used. The codon optimization was necessary to ensure robust expression of the *D. mauritiana corolla* gene in *D. melanogaster* and to circumvent inefficiencies in the CRISPR/Cas9 mediated replacement of the *corolla* gene due to similarities in DNA sequence. The knock-in cassette and homology arms were cloned into the pUC57-Kan vector using sequence and ligation independent cloning and subsequently transformed using a standard protocol. The correct plasmid was selected using colony PCR and sequencing and subsequently used for microinjections into 226 wild-type embryos of the strain *w*^{1118}*hyb5b-8*. 97 G0 males were outcrossed to females with the balancer *X* chromosome *FM7a*. Out of 72 viable crosses, 5 F1 lines were positive for the visible 3xP3 DsRed selection marker. F1 lines were tested for the insertion of the full knock-in cassette by obtaining genomic DNA from single flies and using PCR primers that should only provide an amplicon if the cassette is present. To test the insertion of the cassette in the 5' region, the forward PCR primer is designed to anneal to a region outside of the upstream homology region (5'-G CATGTCCTTGGATGTCAGA) and the reverse primer is designed to anneal to a region within the *corolla* CDS from *D. mauritiana* (5'-GAACTGGGCCATCTGAGTGT). To test the insertion of the cassette in the 3' region, the forward PCR primer is designed to anneal to the Piggy Bac 3' terminal repeat (5'-TTTGACTCACGCGGTCGTTA) and the reverse primer is designed to anneal to a region outside of the downstream homology arm (5'-CTTCTGCTTGAGCA GCTCGT). Samples from two individuals presented with positive amplification of both PCR reactions and no amplification was found in the negative control *w*^{1118}*hyb5b-8*. One of these samples was excised from the agarose gel and via sequencing the correct sequences upstream and downstream were confirmed. To test whether the backbone of the pUC57-Kan vector was inserted into the genome as well, two additional PCR reactions were performed. For the upstream region, the forward primer was designed to anneal to the region outside of the homology arm within the plasmid, i.e. the backbone of the plasmid (5'-CAACT GTTGGGAAGGGCGAT) and the reverse primer from the previous PCR reaction, annealing within the *corolla* CDS from *D. mauritiana*, was reused (5'-GAACTGGGCCAT CTGAGTGT). For the downstream region, the forward primer annealing to the Piggy Bac 3' terminal repeat (5'-TT TGACTCACGCGGTCGTTA) was reused, and the reverse primer was designed to anneal to the downstream region of the homology arm within the plasmid, i.e. the backbone of the plasmid (5'-CATTAGGCACCCCAGGCTTT). No amplification was found in either of the two individuals that were positive for the cassette insertion as well as the negative control *w*^{1118}*hyb5b-8*. Amplification was found from the positive control, the donor plasmid. Positive excision of the selection marker using the Piggy Bac transposase was examined by another PCR reaction using a forward primer annealing to the 3' region of the codon optimized *corolla* CDS from *D. mauritiana* (5'-GGAAGATGAATTCCCGA TGA) and a reverse primer annealing to the downstream homology arm (5'-ACGGCACTTTCGAACTGAAT). All samples showed successful excision of the selection marker as the unexcised line had a larger amplicon and the negative control *w*^{1118}*hyb5b-8* had no amplicon. Via sequencing it was confirmed that one TTAA motif was left in the 3' end of the codon optimized *corolla* CDS from *D. mauritiana* resulting in a silent mutation. Two isogenized and balanced stocks were received from WellGenetics Inc. and the line *w*^{1118}*hyb5b-8*, *corolla*^{mauEx1} was used for crosses to establish the genotypes used in the different experiments.

Chromosome missegregation assay

To assess *X* and *4th* chromosome missegregation, we crossed single virgin female flies of the genotypes y *w/y w; sv*$^{spa-pol}$ (=*corolla*$^{+}$) and y w *corolla*^{mauEx1}/ y w *corolla*^{mauEx1};

sv^{spa_pol} (=$corolla^{mau}$) with males of the genotype *X^Y, ln(1)EN, v f B; C(4)RM, ci* ey^{R}. For experiments at 25 °C, mating was set up for 5 days and progeny was subsequently scored for 8 days from the day of hatching. For experiments at 18 °C, mating was set up for 7 days and adults were moved to fresh vials that were kept at 18 °C for further mating while initial vials were moved to 25 °C for 7 days. Subsequently, progeny was scored for 8 days from the day of hatching. Calculations to determine the percentage of *X* and *4th* chromosome missegregation were performed as before (Zitron and Hawley 1989; Hawley et al. 1992). P values to determine statistical significance were calculated with the Fisher's Exact test.

Recombination assays

To assay recombination on the *X* chromosome we crossed single virgin females of the genotypes *y w/*y^{1} sc^{1} w^{+} cv^{1} v^{1} f^{1} (=$corolla^{+}$) and *y w* $corolla^{mauEx1}$/y^{1} sc^{1} w^{+} cv^{1} v^{1} f^{1} $corolla^{mauEx1}$ (=$corolla^{mau}$) with males of the genotype y^{1} sc^{1} cv^{1} v^{1} f^{1} car^{1}/$B^{S}Y$. For experiments at 25 °C, mating was set up for 5 days and progeny was subsequently scored for 8 days from the day of hatching. For experiments at 18 °C, mating was set up for 7 days, adults were moved to fresh vials that were kept at 18 °C for further mating while vials containing progeny were moved to 25 °C for 7 days. Subsequently, only the female progeny were scored for up to 10 days from the day of hatching for the intervals *sc-cv*, *cv-v*, *v-f*.

To assay recombination on the *2nd* chromosome we crossed single virgin females of the genotypes *y w/y;* net^{1} dpp^{ho} dpy^{ov1} b^{1} pr^{1} cn^{1}/+ (=$corolla^{+}$) and *y w* $corolla^{mauEx1}$/*w* $corolla^{mauEx1}$; net^{1} dpp^{ho} dpy^{ov1} b^{1} pr^{1} cn^{1}/+ (=$corolla^{mau}$) to males of the genotype w^{+}/*Y;* net^{1} dpp^{ho} dpy^{ov1} b^{1} pr^{1} cn^{1}/ net^{1} dpp^{ho} dpy^{ov1} b^{1} pr^{1} cn^{1}. For experiments at 25 °C, mating was set up for 5 days and progeny was subsequently scored for 8 days from the day of hatching. For experiments at 18 °C, mating was set up for 7 days and adults were moved to fresh vials that were kept at 18 °C for further mating while vials containing progeny were moved to 25 °C for 7 days. Subsequently, only the female progeny were scored for up to 10 days from the day of hatching for the intervals *net-dpp*, *dpp-dpy*, *dpy-b*, *b-pr*, and *pr-cn.*

Immunostaining of germaria

For microscopy, germaria of the genotypes *w/w* and *y w/y w; pol* were used as $corolla^{+}$ and there were no differences observed between these. For $corolla^{mau}$ germaria of the genotypes *w* $corolla^{mauEx1}$/*w* $corolla^{mauEx1}$ and *y w* $corolla^{mauEx1}$/*y w* $corolla^{mauEx1}$; pol where also no differences were observed. Germaria were immunostained as in Lake et al. (Lake et al. 2015), except that the samples were incubated with secondary antibodies for 2 h instead of 4 h and mounting was performed in ProLong Glass which was allowed to harden for at least 24 h in the dark at room temperature. Primary antibodies used were affinity-purified rabbit anti-Corolla (1:2000) (Collins et al. 2014), mouse anti-C(3)G 1A8-G2 (Anderson et al. 2005) (1:500), guinea pig anti-Cona (Page et al. 2008) (1:500), mouse anti-lamin Dm0 ADL84.12 (1:100) (Developmental Studies Hybridoma Bank, Iowa), rat anti-CID (1:500) (gift from the Sunkel lab (Martins et al. 2009), rabbit anti-histone γH2AVD pS137 [1:5000] (Rockland Inc., Lot 46042), and mouse anti-Orb 6HA [1:40] (Developmental Studies Hybridoma Bank, Iowa) (Lantz et al. 1994). Secondary antibodies were used at 1:500 and included Alexa Fluor 488 goat anti-mouse (ThermoFisher, A-11001), Alexa Fluor 555 goat anti-rabbit (ThermoFisher, A-21428), Alexa Fluor 647 goat anti-guinea pig (ThermoFisher, A-21450), Alexa Fluor 647 goat anti-mouse IgM (ThermoFisher, A-21238), and Alexa Fluor 594 goat anti-mouse (ThermoFisher, A-11032). DNA was stained with DAPI at a final concentration of 1ug/ml for 10 min.

qPCR

Total RNA from 3 pairs of ovaries per genotype and rearing temperature was isolated in duplicates with a trizol-chloroform extraction. Ovaries were dissected and homogenized in 800 µl of trizol. The homogenized samples were incubated for 5 minutes at room temperature. Then, 0.2 ml of chloroform per ml trizol was added to the samples and the tubes were vigorously shaken by hand for 15 seconds. After an additional incubation at room temperature for 2–3 min, the samples were centrifuged at 12,000xg for 15 minutes at 2–8 °C. The upper aqueous phase, containing the RNA, was carefully pipetted into new tubes. Next, the RNA was precipitated by adding 0.5 ml isopropyl alcohol per initial 1 ml trizol into the aqueous phase. The samples were incubated for 10 minutes at room temperature and subsequently centrifuged at 12,000xg for 10 minutes at 2–8 °C. The supernatant was carefully removed, and the gel-like RNA pellet was washed with 75% ethanol (at least 1 ml of 75% ethanol per initially used 1 ml of trizol). The pellets and ethanol were mixed via vortexing and centrifuged at 7,500xg for 5 minutes at 2–8 °C. Lastly, as much ethanol as possible was removed and the pellets were air dried. Once all the ethanol evaporated, the RNA pellet was dissolved in 20–40 µl of DEPC treated water. The solution was incubated at 55 °C for 5–10 minutes to ensure the complete dissolving of the RNA pellet. The quality of the RNA was assessed via Qubit quantification and using the RNA mini bioanalyzer chip. cDNA was synthesized from total RNA using the SuperScript™ IV VILO™ Master Mix with ezDnase for RT-PCR

using random hexamers. Using the Tecan Freedom Evo (Tecan Life Sciences) to prepare the plates, each genotype was run in triplicate on the QuantStudio 7 (ThermoFisher) using Quanta Biosciences PerfeCTa SYBR Green FastMix ROX reagent. No RT controls were run for every experiment. Primers used were the following: For *corolla*$^{+}$ the primer pair was designed so that at least one primer spanned an intron. Primers were 5'- CAGCTCGAGAAGGAACT CAAGA-3' and 5'- CCAAACGCGGCCCTACAA-3'. For *corolla*$^{+}$ the primers were 5'- ACCCGCTGGTAACAGAG TTC-3' and 5'- CGTTTTCGCAGCTCGTTCTC-3'. For a housekeeping gene ACT42A (FBgn0000043) was used and the primers were 5'- TGGACAGGTCATCACCATCGGA AA-3' and 5'-TTGTAGGTGGTCTCGTGAATGCCA-3'. Data was analyzed using the ΔΔCq method and statistical significance was tested using a two-tailed student's t-test.

Fertility assessment

To assess fertility at 25 °C, mating was set up for 5 days and all progeny were scored for 8 days after hatching. At 18 °C, mating was set up for 7 days and all progeny were counted for up to 10 days. A Mann-Whitney test was used to test statistical significance.

Imaging and image analysis

Structured illumination microscopy

Structured Illumination Microscopy (SIM) was performed with a 63x, N.A 1.40 Plan-Apo oil objective on a ZEISS Elyra 7 microscope. Alexa Fluor 647 signal was excited with 5% laser power for 100 ms, Alexa Fluor 555 signal was excited with 3% laser power for 80 ms, Alexa Fluor 488 signal was excited with 3% laser power for 50 ms, and DAPI signal (405 nm) was excited with 15% laser power for 100 ms. Images were taken with a z-stack size of 1.0 nm z-stack size and 15 phases. Images were then processed with the SIM tool in the Zeiss software. The parameter was set to "adjust" and the sharpness was set to 10.5 for the channels 647, 568, and 488 and set to 3 for the 405 channel. The method was set to "best fit".

Stimulated emission depletion imaging and SC width measurement

Stimulated Emission Depletion (STED) imaging was performed with a 100x, N.A. 1.40 oil objective on a Leica Sp8 Gated STED microscope. Alexa Fluor 594 signal was excited with a pulsed white light laser (80 MHz) tuned to 594 nm with 8% laser power. The pinhole was set to 0.6 Airy unit (AU) and nuclei were zoomed onto with a factor of 12.5. The z step size was set to 0.14 nm. The signal was depleted with a pulsed STED 775 nm laser at 90% power and the delay time between excitation and depletion was set to 600 ns. Images were acquired in 2D mode and averaged 8 times using the line average mode. Emission photons were detected with an internal Leica HyD hybrid detector with a time gate between 0.6 and 6 ns.

Raw images were deconvolved using the Huygens professional deconvolution software (version 22.04). The width of C(3)G was measured following the method described by Billmyre and Cahoon et al. (Billmyre et al. 2019). Well-defined SC regions that were roughly parallel to the xy plane were manually selected, and intensity profiles were obtained by averaging across a three-pixel-wide stripe oriented perpendicular to the SC. For C(3)G distance measurements, these profiles were fitted with double Gaussian functions, and the distance between the two peak positions was calculated.

Widefield imaging on deltavision microscopy system

Images with γH2Av, Orb, and CID staining were acquired on an inverted DeltaVision microscopy system (GE Healthcare) with an Olympus 100× objective (UPlanSApo 100×, NA 1.40) and a high-resolution.

CCD camera or an Applied Precision OMX Blaze microscope equipped with a PCO Edge sCMOS camera. Images were deconvolved prior to analysis using SoftWoRx v. 7.2.1 (Applied Precision/GE Healthcare) software.

Scoring of γH2av foci, CID foci, PCs, disassembly, and fragmentation

γH2Av foci were scored on germaria stained with C(3)G, γH2Av, and Orb. Specifically, for early pachytene, nuclei from different parts of this region were scored and usually more than one early pachytene nucleus per germarium was scored. In early-mid pachytene, if one of the nuclei presented with Orb accumulation, this nucleus was scored. If that was not the case and both nuclei were unobstructed, both were scored. Equally, in mid pachytene, the Orb selected nucleus was scored. To score the number of γH2Av foci, the region of interest (the nucleus) was copied and foci were marked throughout the Z slices as they appeared.

Scoring of CID foci was completed using ImageJ v.1.54f software with minimal brightness and contrast adjustment for ease of foci visualization.

To score the occurrence of PCs and disassembly, SIM images were manually scored for each region (early pachytene, early-mid pachytene, mid pachytene) for the number of PCs relative to numbers pro-oocytes at the distinct stage

as well as how many PCs contained or did not contain C(3)G.

Disassembly was also scored with SIM images by counting pro-oocytes with visibly disassembling SC at distinct stages. Whether SCs were scored as "disassembling" was based on thread continuity and diffuse staining signal.

Fragmentation was scored in maximum projected and deconvoluted STED images. C(3)G thread continuity was used to judge the degree of fragmentation.

AlphaFold3 prediction

Two sequences of Corolla from *D. melanogaster* and *D. mauritiana* were entered into AlphaFold3 and the predictions were made with standard settings. The highest confidence model was opened in ChimeraX and the AlphaFold pLDDT b-factor colors were applied. A scale bar was added.

Figure preparation

For figure preparation of SIM and STED images, the region of interest was selected and duplicated. The duplicated image was z projected with the maximum projection setting. The brightness and contrast were minimally adjusted to ensure proper visualization of the SC and PCs. Channels were then split and lookup tables were applied to specific channels (see figure legends for figure-specific information on lookup tables). Scale bars of 2 µm were added to the C(3)G channel. Graphs were prepared using Prism 10. Figures were put together using Adobe Illustrator.

Results

The C-terminus of Corolla shares sequence features with SYP-4 in *C. elegans* and SIX6OS1 in vertebrates

Previously, three regions of potential sequence homology between Corolla and SYP-4 were reported (Collins et al. 2014). Upon further investigation of the protein and its sequence, we found additional similarities to SYP-4 in *C. elegans* and SIX6OS1, which were recently suggested to be orthologs (Köhler et al. 2025; Neves et al. 2025). The C-terminus of both proteins is rich in phenylalanine compared to the entire protein sequence, and both proteins feature LC3-interacting region (LIR) motifs. Neves et al. (Neves et al. 2025) and (Köhler et al. 2025) report that specific perturbations within the SYP-4 C-terminus significantly disrupt the regulation of crossover formation. We therefore investigated whether *Drosophila* Corolla is a SIX6OS1 ortholog and found that the C-terminus was indeed enriched with phenylalanine. In *D. melanogaster*, 10% of the last 89 amino acids of Corolla were phenylalanine, compared to 4% in the entire protein sequence. Similarly, in *D. mauritiana* Corolla 9% of the last 89 amino acids were phenylalanine compared to 4% in the entire amino acid sequence. Additionally, we found two LIR motifs in Corolla protein sequences from *D. melanogaster* and its *D. mauritiana* ortholog using the Eukaryotic Linear Motif (ELM) resource for functional sites in proteins (Supplementary Fig. 1) (Kumar et al. 2024). One of these motifs is shorter by two amino acids in *D. melanogaster*, which means that through the gene replacement, this motif was extended, and it additionally contains 3 amino acid substitutions. One of these is an amino acid substitution of a phenylalanine with an aspartic acid at the aligned residue 351 (residue 349 in the *D. melanogaster* protein sequence). Phenylalanines in LIR motifs were shown to have a special functional importance in SYP-4 (Neves et al. 2025) but the importance of this one single phenylalanine is unknown. In combination with the previously highlighted homology regions between SYP-4 and Corolla (Collins et al. 2014) it is likely that Corolla is the *Drosophila* ortholog of SIX6OS1.

Replacing the *corolla* gene in *D. melanogaster* with its ortholog from *D. mauritiana* to create a hypomorphic allele

To circumvent the problem of identifying conserved amino acid motifs that we could target for the creation of a hypomorphic allele, we chose to replace the *D. melanogaster* gene encoding the central region protein, Corolla, with that of a close relative. The closest relatives of *D. melanogaster* are *D. mauritiana*, *D. simulans*, and *D. sechellia* (Fig. 1b). Previous studies of recombination in *D. mauritiana* and *D. simulans* revealed that the total map length of *D. mauritiana* was 1.36 (Hawley et al. 2025) to 1.8 (True et al. 1996) times more compared to *D. melanogaster*, and the total map length of *D. simulans* was 1.3 times more compared to *D. melanogaster* (True et al. 1996). Both species exhibit more recombination in the regions proximal to the centromere than *D. melanogaster* (True et al. 1996; Hawley et al. 2025), but the strongest effect was seen in *D. mauritiana*. Therefore, we chose *D. mauritiana* as the donor for the replacement of the endogenous *corolla* gene in *D. melanogaster*, as it would allow us more easily to understand whether Corolla is directly involved in these differences of crossover patterning.

The amino acid sequence of Corolla from *D. mauritiana* shares 86.7% sequence identity with *D. melanogaster* Corolla (Supplementary Fig. 2 and Supplementary file 1). In total, there are 74 amino acid differences including a two amino acid gap (Supplementary Fig. 2 and Supplementary file 1). These amino acid differences have a similarity of

4.7%, meaning that a substituted amino acid is of similar chemical type. The DeepCoil2 program (Zimmermann et al. 2018; Ludwiczak et al. 2019; Gabler et al. 2020) indicates that Corolla from *D. mauritiana* has an overall higher probability for coiled-coil formation within the first 200 amino acids of the protein than *D. melanogaster* (Supplementary Figs. 3a-b). To form coiled-coils, a heptad repeat of seven amino acids must be present, usually denoted as a-b-c-d-e-f-g (McLachlan and Stewart 1975). The positions a and d within that heptad repeat are typically hydrophobic amino acids while positions e and g are typically charged or polar amino acids (McLachlan and Stewart 1975; Parry 1982; Lupas et al. 1991). The higher probability of coiled-coil formation in Corolla from *D. mauritiana* is likely because DeepCoil2 finds more residues fitting the above-described a and d positions of heptad repeats within the first 200 amino acids (Supplementary Figs. 3a-b). Importantly, the length of the region with coiled-coil probability is predicted to be of the same length within the first 200 amino acids of the proteins, and the arrangement of individually predicted coiled-coil domains is largely similar in spacing (Supplementary Figs. 3a-b). This is reminiscent of the findings by Kursel et al. which showed that within nematodes the length and location of coiled-coil domains is highly conserved as well as the overall protein lengths of orthologous SC proteins (Kursel et al. 2021). Indeed, the overall length of the Corolla protein from both *Drosophila* species is strikingly similar with 554 amino acids in *D. melanogaster* and 556 amino acids in *D. mauritiana* (Supplementary Figs. 2–3 and supplementary file 1). In contrast, AlphaFold3 predictions of a Corolla homodimer from *D. melanogaster* shows a distinctly longer coiled coil (approx. 200 A) than from *D. mauritiana* (approx. 300 A) (Supplementary Fig. 4). It is unclear how exactly this may affect Corolla and its interaction partners.

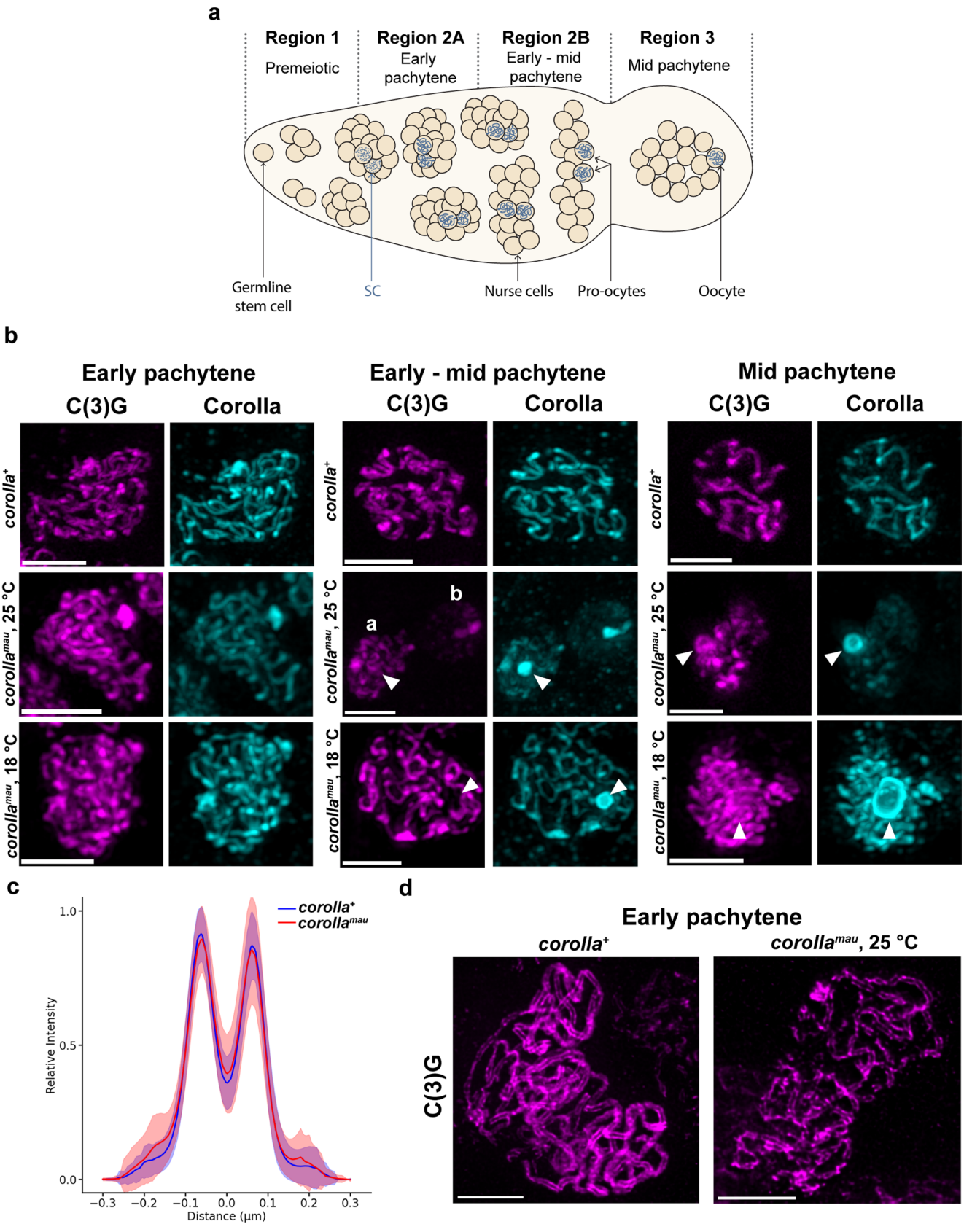
In addition to a higher probability of coiled-coil formation, we also find that Corolla from *D. mauritiana* has a slightly larger intrinsically disordered region (IDR), as well as a small additional IDR within the C-terminus of the protein that is not found in Corolla from *D. melanogaster* according to an InterProScan (Supplementary Figs. 3C-D) (Blum et al. 2025). Specifically, the IDR in Corolla from *D. melanogaster* spans amino acids 308–432 while the first IDR in Corolla from *D. mauritiana* spans amino acids 305–462, and the second small IDR spans amino acids 476–495 (Supplementary Fig. 3c-d). IDRs have been established as important factors in the function of SC proteins. Especially in SYP-4 of *C. elegans*, it is the IDR that is important for the regulation of crossovers and maintenance of biophysical characteristics of the SC (Köhler et al. 2025; Neves et al. 2025). Importantly, IDRs and coiled-coil domains are implicated in promoting phase-phase separation through multivalent interactions (Zhang et al. 2020; Kursel et al. 2021).

Fig. 2 The *corolla*^{mau} gene replacement causes SC maintenance defects. (**a**) Schematic of the *D. melanogaster* germarium. Germline stem cells are found in the premeiotic region 1. These proliferate to a 16-cell cyst at region 2 A where two nuclei enter meiosis and assemble the SC in early pachytene and the remaining nuclei become nurse cells. As these cysts migrate along the germarium, they enter early-mid pachytene in region 2B where we still see two meiotic pro-oocyte nuclei. At mid pachytene, region 3, only one meiotic cell remains, the oocyte. The full-length SC is clearly visible from early pachytene to mid pachytene. (**b**) Immunofluorescence staining of the *corolla*$^{+}$ and *corolla*^{mau} SC. In early pachytene, SC threads of both C(3)G (magenta) and Corolla (cyan) are present in *corolla*$^{+}$ and *corolla*^{mau}. In early-mid pachytene, SC threads of C(3)G and Corolla are visible for *corolla*$^{+}$ and *corolla*^{mau} reared at 18 °C. At the same stage, in *corolla*^{mau} reared at 25 °C the SC is visibly disassembling (**a**) or has already disassembled (**b**). In mid pachytene, SC threads are visible in *corolla*$^{+}$ and *corolla*^{mau} reared at 18 °C, but the SC in *corolla*^{mau} flies reared at 25 °C is in the process of disassembling. Polycomplexes are visible in *corolla*^{mau} nuclei regardless of rearing temperature (marked by arrowheads). Scale bars represent 2 µm length. (**c**) Relative fluorescence intensity of the two C-terminal C(3)G tracks over distance in *corolla*$^{+}$ and *corolla*^{mau} reared at 25 °C. The SC widths between *corolla*$^{+}$ and *corolla*^{mau} are not statistically significantly different. (**d**) Deconvoluted maximum projection of the SC in *corolla*$^{+}$ and *corolla*^{mau} imaged with STED microscopy. The two tracks of the C(3)G C-terminal antibody staining are visible. In *corolla*^{mau}, SC mild fragmentation is visible. Scale bars represent 2 µm length

In light of the differences in protein architecture described above and the high possibility of Corolla being a SIX6OS1 ortholog, we hypothesized that replacing *D. melanogaster* Corolla with its ortholog from *D. mauritiana* would allow for synapsis but could impact recombination. To generate *D. melanogaster* flies expressing the *D. mauritiana* Corolla protein, we used CRISPR/Cas9 to excise *corolla* exons 1–4 and inserted the codon-optimized coding sequence (CDS) of *D. mauritiana corolla* (Fig. 1c). We wanted to insert the CDS in the endogenous *corolla* locus so that regulatory elements of *corolla* gene expression could act on the gene expression of the replacement. We also chose not to insert the introns from *D. mauritiana* to avoid problems caused by foreign intron sequences. The resulting allele, *corolla*^{mau}, was then subjected to detailed phenotypic analysis.

corolla^{mau} females exhibit early SC disassembly

Upon completion of the gene replacement, we first asked how this affected SC assembly, maintenance and disassembly. Within the germarium of *D. melanogaster*, meiotic progression can be followed spatially (Fig. 2a). Using structured illumination microscopy (SIM) on *corolla*^{mau} mutant germaria maintained at 25 °C, we observed that the SC assembled but was not maintained beyond early pachytene (Fig. 2b). Specifically, compared with wild-type controls (=*corolla*$^{+}$) we observed early SC disassembly in 4/37 nuclei in early pachytene, 14/20 nuclei in early-mid pachytene, and 3/3 of nuclei in mid pachytene (Supplementary Fig. 5). To test whether the SC width was affected


a
Region 1
Premeiotic
Region 2A
Early pachytene
Region 2B
Early - mid pachytene
Region 3
Mid pachytene
Germline stem cell
SC
Nurse cells
Pro-ocytes
Oocyte
b
Early pachytene
Early - mid pachytene
Mid pachytene
C(3)G
Corolla
corolla+
corollamau, 25 °C
corollamau, 18 °C
a
b
c
corolla+
corollamau
Relative Intensity
Distance (µm)
d
Early pachytene
corolla+
corollamau, 25 °C
C(3)G

in *corolla*^{mau} mutants we turned to stimulated emission depletion (STED) microscopy, which offers higher resolution than SIM. We used a C(3)G antibody that recognizes a region in the C-terminal globular domain of C(3)G (Anderson et al. 2005). As the C-terminal region of C(3)G is localized in proximity to the lateral elements (Anderson et al. 2005; Cahoon et al. 2017), the fluorescence signal should clearly resolve into two tracks. The two tracks of C(3)G in both *corolla*$^{+}$ and *corolla*^{mau} mutants were clearly visible in the STED images (Fig. 2d). We found that the SC width in *corolla*^{mau} germaria was not significantly different (124 ± 16 nm) compared to the *corolla*$^{+}$ SC (124 ± 9 nm) as determined with a t test (p-value = 0.95) (Fig. 2c). STED microscopy did reveal that only 14% of SCs in early pachytene were full-length while 64% of SCs already showed mild fragmentation, and 21% of SCs show high levels of fragmentation (Supplementary Fig. 6). By early-mid pachytene, 70% of SCs were mildly fragmented while the remaining 30% were highly fragmented (Supplementary Fig. 6). The fact that fragmentation was apparent with STED but not SIM is likely due to the above-mentioned differences in the resolution of these microscopy techniques. Combined, these results show that that the replacement of Corolla from *D. melanogaster* with its ortholog from *D. mauritiana* allowed for the assembly of the SC, but that it could not be maintained beyond early pachytene, when SC fragmentation was already apparent.

SC-dependent centromere clustering in *corolla*^{mau} mutants

In *D. melanogaster*, the SC at the centromeres is different from the chromosome arms. Electron microscopy studies revealed that the central element has a less definite morphology and the lateral elements are surrounded by highly condensed chromatin making it more difficult to distinguish them from each other (Carpenter 1975). In addition, at the beginning of prophase I the centromeres cluster into one or two masses (Takeo et al. 2011). This process is called centromere clustering and requires the presence of C(3)G, Corolla, and Cona (Takeo et al. 2011; Collins et al. 2014). Due to the observed early disassembly and SC fragmentation, we questioned whether centromere clustering would be affected in *corolla*^{mau} flies. To analyze this, we stained germaria with an antibody against CID (Centromere Identifier, the *Drosophila* equivalent of CENP-A) and scored the number of clusters per nucleus (Supplementary Fig. 7). In early pachytene, the average number of CID clusters was 1.9 ± 0.8 for *corolla*$^{+}$ and 1.8 ± 0.7 for *corolla*^{mau} (Supplementary Fig. 7). In early-mid pachytene, the average number of CID clusters was 1.9 ± 0.6 for *corolla*$^{+}$ and 2.1 ± 0.8 for *corolla*^{mau} flies (Supplementary Fig. 7). Lastly, in mid pachytene, the average number of CID clusters was 1.8 ± 0.5 for *corolla*$^{+}$ and 2.1 ± 0.7 for *corolla*^{mau} females (Supplementary Fig. 7). P values determined with an unpaired t-test indicated no statistical significance in any of these cases (Supplementary Fig. 7). Therefore, we can conclude that SC-dependent centromere clustering is not affected in *corolla*^{mau} mutants (Supplementary Fig. 7). This shows that while Corolla from *D. mauritiana* causes defects with SC maintenance, other functions of Corolla like centromere clustering can be successfully completed.

Polycomplexes in *corolla*^{mau} flies do not consist of all SC protein components

In addition to the assembly of the tripartite SC that is not properly maintained, we noted the occurrence of polycomplexes (PC) in *corolla*^{mau} flies (Fig. 2b). PCs are structures consisting of SC proteins that assemble into repetitive structures that resemble the fine ultrastructure of the canonical SC (reviewed in (Hughes and Hawley 2020). While these are most often seen in mutant backgrounds that perturb the SC, well-studied examples of PCs include those induced by increased temperature in wild-type organisms (Bilgir et al. 2013; Rog et al. 2017). The spontaneous occurrence of PCs under standard conditions has also been reported, but it is not a common phenomenon (Anderson et al. 2005; Hughes and Hawley 2020). In *corolla*^{mau} mutant germaria, 1/37 pro-oocytes at early pachytene, 15/18 pro-oocytes at early-mid pachytene, and 3/3 oocytes at mid pachytene contained PCs, which were not observed in *corolla*$^{+}$ (Fig. 2b and Supplementary Fig. 8a). Importantly, we found that 61% of PCs in *corolla*^{mau} flies lacked the SC component C(3)G (Fig. 2b and Supplementary Figs. 8a-b). To our knowledge, PCs in flies usually consist of all SC central region proteins (Hughes and Hawley 2020), which would make this the first observation of PCs lacking a central region component. The PCs are torroidal and appear hollow (Fig. 2b and Supplementary Figs. 8b-c). With this shape, the PCs are reminiscent of those seen in the *c(3)g*^{Cdel} mutants reported by Jeffress et al. (Jeffress et al. 2007), as well as *sina*^{A4}/*sina*^{Df} mutants reported by Hughes et al. (Hughes et al. 2019). However, all previously reported PCs contain C(3)G. To verify that the PCs were localized within the nucleus, we co-stained for the nuclear envelope protein Lamin and found that they were indeed nuclear (Supplementary Fig. 8c).

To summarize, we found that the replacement of *D. melanogaster* Corolla with its ortholog from *D. mauritiana* results in abnormal PC formation. Some of these PCs do not contain the transverse filament protein C(3)G, something that has never been observed before in flies. PCs may form due to the early disassembly of the SC, whereas the PCs lacking C(3)G may indicate a faulty interaction

between C(3)G from *D. melanogaster* and Corolla from *D. mauritiana.*

The *corolla*^{mau} SC maintenance defect is temperature-sensitive

Due to the occurrence of PCs, and especially those without the transverse filament protein C(3)G, we wondered whether the observed SC disassembly was caused by an unstable interaction between *D. mauritiana* Corolla and the native *D. melanogaster* proteins Cona and C(3)G. Corolla and Cona have been previously shown to interact with each other in a yeast two-hybrid assay (Collins et al. 2014). Importantly, it is still unclear how these two proteins interact with C(3)G.

Previous studies have linked the formation of PCs with elevated temperature in several plant species and *C. elegans* (Higgins et al. 2012; Bilgir et al. 2013). As the PCs observed in *corolla*^{mau} mutants always contained Corolla and Cona, we infer that their interaction was not disrupted. While 25 °C is the standard rearing temperature for both *D. melanogaster* and *D. mauritiana*, we hypothesized that the 74 amino acid changes in *D. mauritiana* Corolla could destabilize its interaction with *D. melanogaster* C(3)G and Cona in a temperature-dependent manner. Hydrophobic multivalent interactions have been shown to be important for phase-phase separation (Rog et al. 2017; Zhang et al. 2020; Kursel et al. 2021), and a lowering of temperature leads to a reduction of molecular motion and the stabilization of condensates (Jeon et al. 2025). Therefore, we asked if rearing *corolla*^{mau} mutants at 18 °C could rescue the early disassembly phenotype and the occurrence of PCs. Indeed, early SC disassembly was not observed in *corolla*^{mau} flies reared at 18 °C (Fig. 2b and Supplementary Fig. 9). Notably, PC formation was still observed in these germaria. Specifically, we observed PCs in 6/34 pro-oocytes at early pachytene, 8/13 at early-mid pachytene, and 2/2 at mid pachytene (Supplementary Fig. 8a). Interestingly, while the ratio of PCs with and without C(3)G was 39:61 (9/18 PCs for each type) for *corolla*^{mau} reared at 25 °C, for those reared at 18 °C we observe that only 3/19 PCs contain C(3)G while 16/19 PCs did not (Supplementary Fig. 8a). From this we conclude that the formation of PCs is not caused by early SC disassembly in *corolla*^{mau} mutants reared at 25 °C. We further observed fewer C(3)G-positive PCs in *corolla*^{mau} females reared at 18 °C. This may suggest that Corolla from *D. mauritiana* and Cona from *D. melanogaster* are prone to form PCs with each other, but as the SC is not disassembling early at 18 °C, C(3)G is not readily available to join the PCs.

As an alternative explanation for the formation of PCs in *corolla*^{mau} mutant germaria, we compared linear recognition motifs present on the Corolla proteins from *D. melanogaster* and *D. mauritiana* using the ELM resource for functional sites in proteins (Supplementary Table 1) (Kumar et al. 2024). Important to note here is that the *corolla* gene theoretically encodes for two isoforms of Corolla with only a three amino acid difference (Supplementary Fig. 10). Currently, it is unclear whether both isoforms are expressed, and functional studies should help clarify this. We also do not know which of the linear motifs mentioned below are functionally important for Corolla and the SC. Corolla isoforms A and B in *D. melanogaster* contain five and six functional sites, respectively, that are unique to the *D. melanogaster* protein. Candidates that could potentially create problems are the absence of a COP1 E3 ligase binding degron motif, a SUMO interaction site (both found on isoform A and B), as well as an APC/C destruction box motif (only on isoform B) on the Corolla protein from *D. mauritiana* (Supplementary Table 1). The lack of these motifs may affect transcriptional regulation and protein degradation. Importantly, the gene *sina* also codes for an E3 ligase. While the *sina* mutants studied in Hughes et al. are mutations in the gene body (Hughes et al. 2019), the lack of the required motif in the degradation target would likely also result in functional problems. In the Corolla protein of *D. mauritiana* there are two unique motifs, one of which is an additional motif for the deubiquitinase Usp7. While it was shown that the knockdown of Usp7 has detrimental effects on SC maintenance, recombination, and fertility (Lake et al. 2024), it is unclear what effects an additional Usp7 motif would have. To understand whether any of these differences in linear recognition motifs may lead to changes in how *corolla* is expressed in *corolla*^{mau} flies, we turned to quantitative polymerase chain reaction (qPCR). We did find a 19-fold overexpression of *corolla* in *corolla*^{mau} flies reared at 25 °C and a 12-fold overexpression in *corolla*^{mau} flies reared at 18 °C (Supplementary Fig. 11). The difference between *corolla*^{mau} flies reared at both temperatures was not statistically significant (Supplementary Fig. 11). Previously, it has been shown that the overexpression of *corolla*, achieved by the insertion of additional gene copy numbers, leads to the formation of PCs (Feijão et al. 2022). However, the morphology of the PCs reported by us compared to Feijão et al. is quite different. While our observed PCs were toroidal and hollow and started appearing in early pachytene, PCs reported by Feijão et al. are elongated filaments that begin forming as the SC disassembles in diplotene (Feijão et al. 2022). We cannot exclude that the overexpression of *corolla*^{mau} is linked to any of our observed phenotypes because the regulation of *corolla* gene expression has not been systematically studied. Further research will be needed to investigate the functional consequences of *corolla* overexpression at similar levels.

Chromosome segregation and recombination are significantly affected in *corolla*^{mau} females

Given the effects on SC assembly, we next tested how the *corolla* gene replacement affected fertility. For this, we assessed the number of eclosed progeny from 10 females per genotype and rearing temperature in their first week. While flies at 18 °C overall had less progeny, no statistically significant differences were found when we compared *corolla*^{mau} flies to *corolla*$^{+}$ flies reared at the same temperature (Supplementary Fig. 12). The reduction of progeny in flies reared at the lower temperature is expected due to slower oocyte development. After this, we assessed the effects on chromosome segregation and recombination. In *corolla*^{mau} flies, *X* chromosome missegregation increased significantly (Fig. 3a and Supplementary Fig. 13a). This effect was slightly less pronounced in flies reared at 18 °C (8.5% vs. 10.8% at 25 °C), but the difference was not statistically significant (Fig. 3a and Supplementary Fig. 13a). Importantly, at either temperature the rate of *X* chromosome missegregation was drastically lower than the 44.5% reported in *corolla* null mutant flies (Collins et al. 2014). *4th* chromosome missegregation was significantly lower in *corolla*$^{+}$ flies reared at 18 °C compared to 25 °C but, surprisingly, *corolla*^{mau} females did not show significant differences compared to *corolla*$^{+}$ females (Fig. 3a and Supplementary Fig. 13a). This suggests that the proper segregation of the *4th* chromosome in control females was improved at 18 °C compared to 25 °C. We would therefore have expected to see an increase in *4th* chromosome missegregation in conjunction with the increase in *X* chromosome missegregation in *corolla*^{mau} mutants. The small and mostly heterochromatic *4th* chromosome in *D. melanogaster* is, with very few exceptions, achiasmate and segregates via the distributive system (reviewed in (Scott Hawley and Theurkauf 1993; Hartmann and Sekelsky 2017). The distributive system also ensures the proper segregation of any additional achiasmate chromosomes (Scott Hawley and Theurkauf 1993). Typically, with an increase in achiasmate chromosomes (e.g. through a mutant SC allele), *4th* chromosome missegregation is reported at half to two thirds level of *X* chromosome missegregation (Page et al. 2007; Collins et al. 2014; Hughes et al. 2019). This arises because the distributive system gets overloaded with achiasmate chromosomes and fails to segregate the *4th* chromosome. In *corolla*^{null} flies for example, *X* chromosome missegregation was 44.5% and *4th* chromosome missegregation was 30.0% (Collins et al. 2014). It therefore remains unclear why *4th* chromosome missegregation is not affected in *corolla*^{mau} flies.

Due to the elevated *X* chromosome missegregation in *corolla*^{mau} flies, we next hypothesized that recombination would be significantly reduced due to the gene replacement. Considering that the rate of *X* chromosome missegregation in *corolla*^{mau} mutants was not significantly different between the different rearing temperatures, we further hypothesized that recombination would be decreased to a similar extent in *corolla*^{mau} flies reared at 18 °C and 25 °C. Indeed, *X* chromosome recombination was significantly affected by the gene replacement (Fig. 3b and Supplementary Fig. 13b). In *corolla*^{mau} flies reared at 25 °C, all intervals scored for recombination across the *X* chromosome had dramatically reduced levels of recombination (Fig. 3b and Supplementary Fig. 13b). The reduction in crossing over ranged from 5% of the *corolla*$^{+}$ map length for the interval *cv-v* to 26% of the *corolla*$^{+}$ map length in the interval *v-f* (Fig. 3b and Supplementary Fig. 13b). In contrast, *corolla*^{mau} flies reared at 18 °C had significantly higher levels of recombination in two intervals (65% of the *corolla*$^{+}$ map length in *cv-v* and 81% of the *corolla*$^{+}$ map length in *v-f*) than *corolla*^{mau} flies raised at 25 °C (Fig. 3b and Supplementary Fig. 13b). In the interval *sc-cv*, however, recombination was still significantly lower than in *corolla*$^{+}$ with 10% of the *corolla*$^{+}$ levels (Fig. 3b and Supplementary Fig. 13b). Over the entire scoring interval on the *X* chromosome, *corolla*^{mau} flies reared at both temperatures had significantly reduced levels of recombination. Specifically, *corolla*^{mau} flies reared at 25 °C had only 15% of the *corolla*$^{+}$ *X* chromosome map length and those reared at 18 °C only 61% (Fig. 3b and Supplementary Fig. 13b). Interestingly, *corolla*$^{+}$ flies reared at 18 °C had a significantly longer total map length (Fig. 3b and Supplementary Fig. 13b), suggesting that crossover interference is decreased at 18 °C compared to 25 °C. This aligns with previously published data showing that recombination in *D. melanogaster*, as well as *A. thaliana*, have a U-shaped response when plotting crossover rates over temperature (Plough 1917; Lloyd et al. 2018). The results for *X* chromosome map lengths are also reflected in the exchange rank frequencies calculated with the Crossover Maximum Likelihood Estimation Tool (Table 1) (Hawley et al. 2025). Exchange rank frequencies provide more accurate information about bivalents with no crossovers (E0), a single crossover (E1), two crossovers (E2), and three crossovers (E3) than the direct readout on crossover chromatid types from scoring crossovers (Miller et al. 2016). *X* chromosome E0 tetrads are highly elevated in *corolla*^{mau} flies kept at both temperatures but values increased dramatically at 25 °C with 0.864 E0 frequency while the *corolla*$^{+}$ E0 frequency is 0.251 (Table 1). It is important to note that as the *corolla* locus is positioned between *cv* and the typical additional marker y^{+} (located on the short arm), the interval *cv*-y^{+} could not be scored, which is why the E0 frequency observed for *corolla*$^{+}$ may seem high compared to previously published data. While *X* chromosome E0 tetrads for *corolla*^{mau} flies at 18 °C are still elevated (Table 1), they

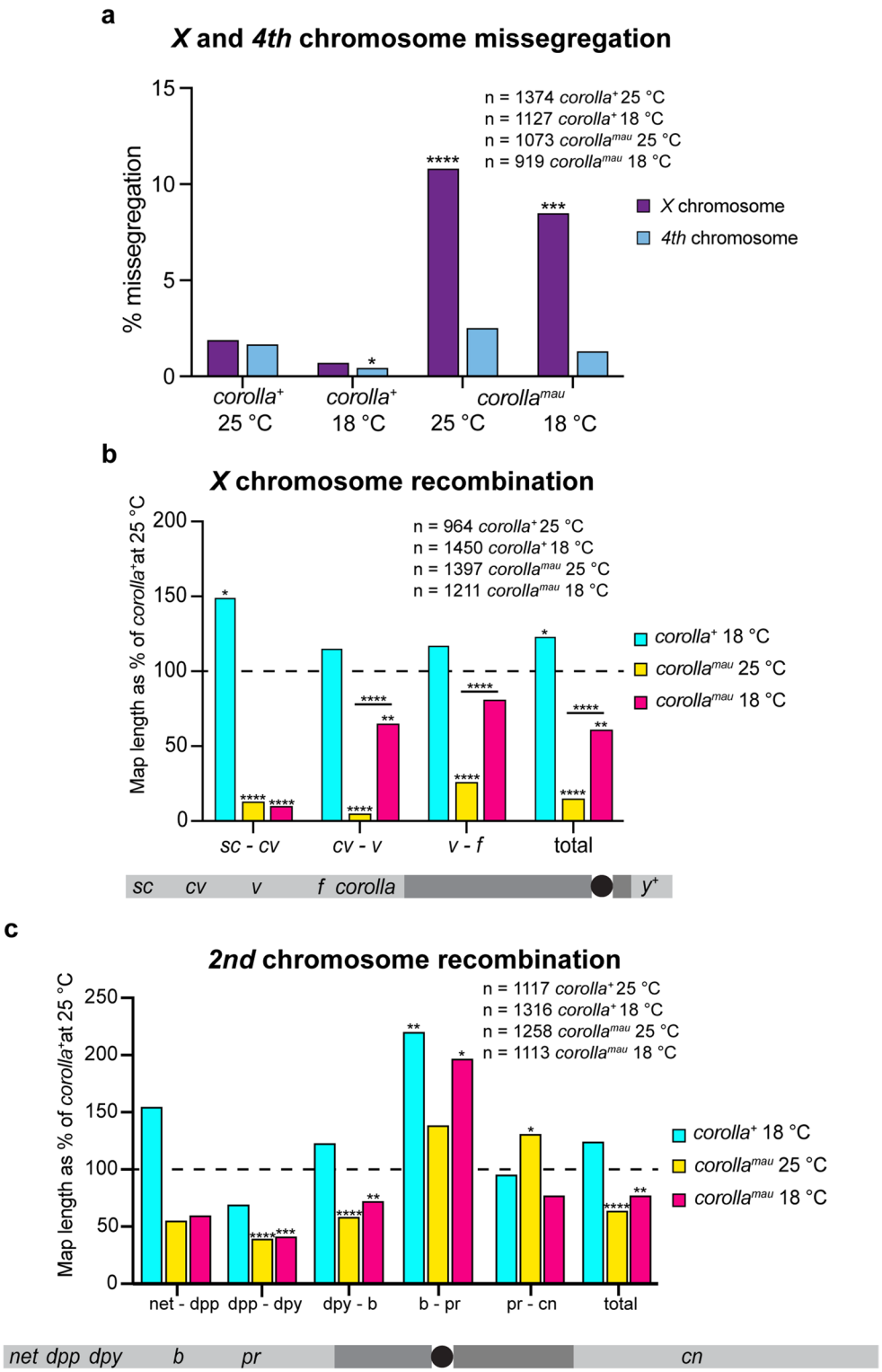


Fig. 3 *corolla*^{mau} females have modest defects in chromosome segregation and recombination. (**a**) *X* and *4th* chromosome missegregation. The percentage of missegregation is plotted for *corolla*$^{+}$ and *corolla*^{mau} kept at both temperatures. (**b**) *X* chromosome recombination. The map length is plotted as a percentage of *corolla*$^{+}$ at 25 °C for each scored interval, as well as the total scored interval. A schematic of the *X* chromosome with the marker genes scored as well as the location of *corolla* and y^{+} is illustrated below the plot. (**c**) *2nd* chromosome recombination. The map length is plotted as a percentage of *corolla*$^{+}$ at 25 °C for each scored interval, as well as the total scored interval. Numbers of scored individual females for each experiment are provided for each genotype and temperature. A schematic of the *2nd* chromosome with the marker genes scored is illustrated below the plot. Statistical significance was calculated by Fisher's exact test. Asterisks on top of bars indicate statistical significance in comparison to *corolla*$^{+}$ at 25 °C. Asterisks on top of horizontal lines indicate statistical significance comparing *corolla*^{mau} at 25 °C to *corolla*^{mau} at 18 °C. * means $p \leq 0.05$, ** means $p \leq 0.01$, *** means $p \leq 0.001$, **** means $p \leq 0.0001$

had significantly more recombination than those at 25 °C (Fig. 3b; Table 1). The fact that *corolla*$^{+}$ flies reared at 18 °C had a significantly longer total map length is reflected in the E0 tetrads being less than for *corolla*$^{+}$ at 25 °C and both E1 and E2 tetrads are increased.

Previously, it has been shown that distinct deletions in the *D. melanogaster* C(3)G coiled-coil region differentially impact recombination rates on the *X* chromosome and the autosomes (Billmyre et al. 2019). We therefore next examined chromosome *2* recombination rates in *corolla*^{mau}

Table 1 Exchange rank frequencies for the *X* and *2nd* chromosomes for *corolla*$^{+}$ and *corolla*^{mau} females at 18 °C and 25 °C. Values were calculated with the crossover maximum likelihood Estimation tool (Hawley et al. 2025)

X chromosome	*corolla*$^{+}$, 25 °C	*corolla*$^{+}$, 18 °C	*corolla*^{mau}, 25 °C	*corolla*-^{mau}, 18 °C
E0	0.251	0.132	0.864	0.523
E1	0.595	0.631	0.133	0.405
E2	0.154	0.237	0.003	0.073
2nd chromosome	*corolla*$^{+}$, 25 °C	*corolla*$^{+}$, 18 °C	*corolla*^{mau}, 25 °C	*corolla*-^{mau}, 18 °C
E0	0.224	0.074	0.515	0.447
E1	0.691	0.817	0.434	0.449
E2	0.078	0.073	0.032	0.090
E3	0.007	0.036	0.019	0.014

mutants. A key difference observed between crossing over on the *X a*nd the *2nd* chromosomes is that there were no significant differences between *corolla*^{mau} flies reared at the two different temperatures in any of the scored intervals (Fig. 3c and Supplementary Fig. 15c). However, there were distinct differences between *corolla*^{mau} and *corolla*$^{+}$ flies in specific scoring intervals. Specifically, in two intervals (*dpp-dpy* and *dpy-b*), *corolla*^{mau} flies reared at either temperature had significantly reduced levels of recombination compared to *corolla*$^{+}$ reared at 25 °C (Fig. 3c and Supplementary Fig. 15c). For the interval *dpp-dpy*, *corolla*^{mau} mutants reared at 25 °C had a map length that was 39% that of the observed map length in *corolla*$^{+}$. In the same interval, the map length for *corolla*^{mau} mutants reared at 18 °C only improved non-significantly to 41% of the *corolla*$^{+}$ map length (Fig. 3c and Supplementary Fig. 15c). Scoring of the interval *dpy-b* of *corolla*^{mau} females reared at 25 °C and 18 °C revealed 58% and 72%, respectively, of the *corolla*$^{+}$ map length. In the interval *b-pr*, *corolla*^{mau} flies reared at 18 °C had significantly higher levels of recombination, as did *corolla*$^{+}$ flies at the same temperature (Fig. 3c and Supplementary Fig. 15c). In the interval *pr-cn*, *corolla*^{mau} flies reared at 25 °C had significantly higher levels of recombination (Fig. 3c and Supplementary Fig. 15c). This is especially interesting because *pr-cn* spans the centromere of chromosome *2*, indicating that crossovers in the region around it have increased. However, we do not know how close these crossovers were to the pericentromeric heterochromatin. Across the entire scoring interval on the *2nd* chromosome, *corolla*^{mau} flies reared at both temperatures had significantly reduced levels of recombination with 64% of the *corolla*$^{+}$ map length for those reared at 25 °C and 77% for those reared at 18 °C (Fig. 3c and Supplementary Fig. 15c). As a result, E0 tetrads for the *2nd* chromosome were elevated for *corolla*^{mau} mutants at both temperatures, accompanied with a large decrease in E1 tetrads in comparison to *corolla*$^{+}$ flies (Table 1). Again, E0 tetrads for *corolla*$^{+}$ flies reared at 18 °C were dramatically reduced compared to those reared at 25 °C (0.074 vs. 0.224), and both E1 and E3 tetrads were increased (Table 1).

With all the above-described differences in recombination in *corolla*^{mau} flies, we wondered whether double-strand break (DSB) formation or their repair were negatively affected. In *D. melanogaster*, DSBs form after synapsis and can be reduced in SC deficient mutants (Jang et al. 2003). We assessed the number of DSBs by counting γH2Av foci, a histone modification found at DSBs (Rogakou et al. 1998). We did not find significant differences in the formation or repair of DSBs between *corolla*$^{+}$ and *corolla*^{mau} (Supplementary Fig. 14). While there was a significant increase in DSBs, regardless of genotype, in flies reared at 18 °C compared to flies reared at 25 °C (Supplementary Fig. 14), this likely reflects a delay in the repair of DSBs at the colder temperature. Importantly, the total number of DSBs formed cannot be visualized in repair-proficient flies due to the dynamic process of DSB formation and repair (Mehrotra and McKim 2005). These findings suggest that recombination changes observed in *corolla*^{mau} flies are not due to differences in DSB formation.

Additionally, we tested whether *corolla*^{mau} germaria showed any sign for pachytene checkpoint activation. For this, we examined Orb localization which by mid pachytene usually only localizes to the cytoplasm of one oocyte. In the case of pachytene checkpoint activation, Orb localizes to two oocytes in mid pachytene (Joyce and McKim 2010). In all germaria of *corolla*^{mau} flies, Orb localized to only one oocyte in mid pachytene, indicating that the pachytene checkpoint does not get activated (Supplementary Fig. 14).

In summary, *X* chromosome missegregation was significantly increased in *corolla*^{mau} mutants compared to *corolla*$^{+}$ regardless of the temperature they were raised in, while *4th* chromosome missegregation was not significantly altered. On the *X* chromosome, a significant improvement in crossover rates was observed in *corolla*^{mau} flies reared at 18 °C compared to those reared at 25 °C, but overall map lengths on the *X* chromosome and the *2nd* chromosome were significantly reduced in *corolla*^{mau} mutants at both temperatures. These data suggest that the distributive system maintains its ability to segregate the *4th* chromosome but sporadically fails to segregate the *X* chromosomes. Further, *corolla*^{mau} flies did not display any defects in DSB numbers nor was the pachytene checkpoint activated. These findings support that firstly, the observed crossover defects were caused by the altered Corolla protein and not by a reduction in the number of DSBs and secondly, the defects were not grave enough to trigger the pachytene checkpoint.

Discussion

The *corolla*^{mau} gene replacement created a hypomorphic mutation

The SC assembles in early meiosis I to connect homologous chromosomes and ensure crossover formation. Most mutations available to research the SC are null alleles that prevent any SC assembly and do not allow for direct studies on how the SC is involved in the process of crossover placement. We found that Corolla is a likely ortholog of the vertebrate protein SIX6OS1 and the *C. elegans* protein SYP-4. By replacing the *corolla* gene in *D. melanogaster* with its ortholog from *D. mauritiana*, we have created the first partial-loss-of-function allele of *corolla*. When reared at 25 °C, these *corolla*^{mau} flies presented with fragmentation and early disassembly of the SC. The early SC disassembly in the *corolla*^{mau} females was rescued by lowering the rearing temperature to 18 °C, indicating that problems in SC maintenance did not arise from irreconcilable incompatibility between Corolla from *D. mauritiana* and C(3)G and Cona from *D. melanogaster*. In addition, we observed PCs in *corolla*^{mau} reared at both temperatures, some of which contain Corolla and Cona but lack the transverse filament protein C(3)G. In accordance with increased rates of *X* chromosome missegregation, the map lengths of the *corolla*^{mau} *X* and *2nd* chromosomes were significantly reduced compared to *corolla*$^{+}$ *X* and *2nd* chromosomes at both rearing temperatures. It is evident that the gene replacement in *corolla*^{mau} flies caused significant recombination defects compared to *corolla*$^{+}$ flies but these defects were not as severe as in the *corolla*^{null} mutant (Collins et al. 2014). Therefore, by replacing the *corolla* allele in *D. melanogaster* with the *corolla* coding sequence from *D. mauritiana*, we established a hypomorphic allele. The partial-loss-of-function becomes strikingly clear in *corolla*^{mau} flies reared at 18 °C. While the SC maintenance defect was rescued at this lower rearing temperature, recombination was still significantly lower than *corolla*$^{+}$ females. This further suggests that the SC and/or the protein Corolla play a role in the regulation of crossover formation.

The SC in *corolla*^{mau} flies is unstable at 25 °C

We have shown that the SC disassembles early in the *corolla*^{mau} germaria at 25 °C, a phenotype that is rescued at 18 °C (Fig. 2b and Supplementary Figs. 5–6). These data suggest that the introduction of Corolla from *D. mauritiana* into the SC with Cona and C(3)G from *D. melanogaster* creates an instability that is intolerable at 25 °C but tolerable at 18 °C. Protein-protein interactions between Corolla and Cona have been shown in the past by yeast two-hybrid assay (Collins et al. 2014), but it is still unclear how or if C(3)G directly interacts with these two proteins. Potentially, some of the 74 amino acid differences between Corolla from *D. melanogaster* and *D. mauritiana* are important for this interaction with C(3)G. The SC has been shown to have features of a biomolecular condensate (Rog et al. 2017) and lower temperatures are known to stabilize biomolecular condensates as hydrophobic interactions are strengthened through a reduction in molecular motion (Jeon et al. 2025). This may explain why the early disassembly of the SC is rescued in *corolla*^{mau} females at 18 °C. One potential explanation is that some of the 74 amino acids are important for the proper establishment of connections within the SC to maintain it. While at 25 °C amino acid differences introduced through the gene replacement may be intolerable and lead to the disassembly of the SC, the interactions could be generally stabilized at the lower temperature of 18 °C, allowing for its proper maintenance.

Unique polycomplexes have been identified in *corolla*^{mau} germaria

We report the first occurrence of PCs in flies that lack the transverse filament protein. Potentially, this tells us how the Corolla protein from *D. mauritiana* interacts with the other SC proteins in *D. melanogaster*. As described above, the coiled-coil domain of Corolla from *D. mauritiana* has an overall higher probability to form such coiled-coils and its IDR is longer compared to Corolla from *D. melanogaster* (Supplementary Fig. 3). While the functional implications of both factors are currently unknown, one hypothesis is that these cause Corolla from *D. mauritiana* to form PCs. Future experiments will be needed to determine the functional impact of the higher probability for coiled-coil formation and longer IDR on PC formation.

Our initial hypothesis was that SC disassembly and the formation of PCs without C(3)G were both caused by an inability to interact with C(3)G. That hypothesis is clearly incorrect. While lowering the rearing temperature rescued SC disassembly, it did not affect total PC number. Instead, we observed an increase in the proportion of PCs without C(3)G. This may be the reason why we did not see C(3)G associating with more PCs in *corolla*^{mau} females reared at 18 °C. Potentially, as the SC is not disassembling, the majority of C(3)G proteins stay within the canonical SC and do not associate with the PCs, while a significant portion of Corolla and Cona proteins do associate in PCs, with or without C(3)G.

Alternative explanations for the formation of PCs are aberrant gene expression regulation or problems in the regulation through other proteins by recognizing linear motifs on the Corolla amino acid sequence. As mentioned above,

we did find that *corolla* in germaria of *corolla*^{mau} females is significantly overexpressed compared to *corolla*$^{+}$ females (Supplementary Fig. 11). While previous research showed that the overexpression of Corolla only lead to PCs linked to SC disassembly in diplotene (Feijão et al. 2022), it is possible that additional dysregulations of gene expression exacerbate previously described phenotypes. Additionally, the functional relevance of linear motifs on Corolla has not been extensively studied. Therefore, it is unknown whether the differences in linear motifs between Corolla in *D. melanogaster* and *D. mauritiana* play a role in the formation of PCs or other phenotypes observed in *corolla*^{mau} females. Future research is needed to elucidate whether any of these motifs or gene expression differences have functional consequences.

Recombination and chromosome missegregation in *corolla*^{mau} females indicate that Corolla plays a role in crossover formation

In *corolla*^{mau} flies reared at 25 °C we see dramatically reduced levels of recombination on the *X* chromosome (Fig. 3b) while *X* and *4th* chromosome missegregation is moderate in comparison to the *corolla*^{null} mutants (Collins et al. 2014) (Fig. 3A). Crossover levels on the *X* chromosome were increased in *corolla*^{mau} females reared at 18 °C, coinciding with the rescue of SC maintenance defects at the standard rearing temperature. These results align with data from the deletions in the coiled-coil region of C(3)G, which suggested that full-length SC is needed from early to early-mid pachytene (Billmyre et al. 2019). As the SC in *corolla*^{mau} germaria reared at 25 °C starts to show fragmentation in early pachytene and disassembles in early-mid pachytene, *X* chromosome recombination is decreased by a great extent.

Importantly, the results for recombination and missegregation seen in *corolla*^{mau} flies are not identical with those reported for *c(3)G* mutants by Billmyre and Cahoon et al. (Billmyre et al. 2019). The early SC disassembly in two of the *c(3)G* partial deletions resulted in significant reductions of *X* chromosome recombination, which coincided with no significant increase in *X* or *4th* chromosome missegregation. This was likely because *X* chromosome crossovers failed to form due to the early disassembly of the SC, while autosomal crossovers were changed in a different manner. The SC disassembly in these partial *c(3)G* deletions leads to improper crossover distribution and specifically a significant increase in centromere proximal crossovers (Billmyre et al. 2019) which was not observed in *corolla*^{mau} females. Directly comparing the values for *X* and *2nd* chromosome crossovers as well as *X* and *4th* chromosome missegregation between Billmyre and Cahoon et al. with results from *corolla*^{mau} females, it becomes strikingly clear that Corolla may play a role in crossover formation in addition to its structural function (Supplementary Fig. 15) (Billmyre et al. 2019). Even in the *c(3)G* partial deletion females with the lowest rates of *X* chromosome recombination (*c(3)G*^{CC3}), *X* and *4th* chromosome missegregation were not as dramatically increased as in *corolla*^{mau} females (Supplementary Fig. 15).

It is important to emphasize that while we established a strong role for Corolla in crossover formation, this process is mediated by many *cis*- and *trans*-acting elements (reviewed in (Sekelsky 2017; Hughes et al. 2018). One noteworthy example is MEI-218, a protein that has previously been shown as highly relevant for crossover formation as *mei-218* mutants have a severe reduction in crossovers while other meiotic processes, i.e. SC assembly and disassembly and DSB formation are unaffected (McKim et al. 1996). In transgenic *D. melanogaster* expressing the *D. mauritiana* gene *mei-218*, crossover numbers were increased specifically in regions proximal to telomeres and centromeres (Brand et al. 2018). These changes recapitulate general trends of crossover patterns observed in *D. mauritiana* while not entirely phenocopying the *D. mauritiana* wild type crossover landscape. Interestingly, the gene replacement of the C(3)G coding gene from *D. mauritiana* to *D. melanogaster* repatterned the crossover landscape more closely to that of *D. mauritiana* (Hughes et al. 2025). To reconcile all these results, we may turn to the coarsening model of crossover formation (reviewed in (Girard et al. 2023). In early meiosis, many more DSBs are formed than will later turn into crossovers (Mehrotra and McKim 2005). Likewise, the number of recombination nodules (RNs), which are sites of protein aggregates that promote crossover formation, decreases throughout prophase I until they correspond with the number and locations of designated crossover sites (Carpenter 1984). According to the coarsening model, this reduction in the number of RNs is mediated by the migration of pro-crossover factors between these nodules along the SC (Morgan et al. 2021; Von Diezmann et al. 2024; Zhang et al. 2025). This means that on the one hand, pro-crossover factors themselves may establish species-specific differences through different protein properties which establish their unique coarsening behavior. On the other hand, SC proteins and how they are organized with each other influences how pro-crossover factors coarsen along the structure. This is exemplified by the above-mentioned *c(3)G* replacement which caused a shortening of the SC width and work showing that a *syp-4* mutant causes a reorganization of SC components coinciding with an increase in crossovers formed (Köhler et al. 2025; Hughes et al.

2025). Thus, many factors are important for the establishment of crossover patterns.

To conclude, null mutations are integral in providing binary answers to questions like: "Is the SC required for crossover formations?" With novel alleles like *corolla*^{mau}, we can now begin to untangle the complexities of the SC's involvement in crossover formation and how the SC functions as a complex. This opens many avenues for future research. The failure to maintain the SC beyond early pachytene at the standard rearing temperature of 25 °C, which is rescued by rearing at 18 °C, opens the possibility that the SC in *corolla*^{mau} females is destabilized due to amino acid differences. Future research could identify which of the 74 amino acid differences between Corolla from *D. melanogaster* and *D. mauritiana* contribute to this instability. For this, further research to understand how Corolla interacts with other SC proteins will be crucial. Further, when *corolla*^{mau} flies are reared at 18 °C, why do we see a decrease in PCs that have C(3)G compared to 25 °C? Is C(3)G simply less readily available to join the PCs with the full-length SC maintained? And importantly, while the SCs ultrastructure is highly conserved across eukaryotes, understanding how its proteins come together and contribute to the crossover landscape will be one of the important questions to answer in the future.

Supplementary Information The online version contains supplementary material available at https://doi.org/10.1007/s00412-025-00839-z.

Acknowledgements We would like to thank Cathleen M. Lake and Stacie E. Hughes for fruitful discussions throughout the project. We would also like to thank Tolkappiyan Premkumar for the discussion that led to our discovery of temperature-sensitive phenotypes in corolla(mau) flies. A very big thank you to Cathleen M. Lake and Stacie E. Hughes for their help with the manuscript and additional thanks to Helen R. Horkan and Kimla J. Virden for feedback on writing. Thanks also go to Angela Miller for the illustration of the synaptonemal complex and germarium. S. W. would also like to thank Amanda Kroesen and Cathy McKinney for assistance with the SIM and STED microscopes respectively. R.S.H was an American Cancer Society Researcher.

Author contributions Conceptualization: R.S.H. Acquisition of data and analysis: S.W. and G.M., Z.Y. performed SC width measurements on STED data. J.G. performed cDNA synthesis and qPCR. C.S. made the mutant fly line and provided technical support. Visualization: S.W., Z.Y. provided graph of SC width measurements. Writing of the manuscript: S.W. Supervision: R.S.H. and M.G. All authors reviewed the manuscript.

Funding The authors did not receive funding support from any external organizations for the submitted work. The authors have no relevant financial or non-financial interests to disclose.

Data availability Original data underlying this manuscript can be accessed from the Stowers Original Data Repository at [https://www.stowers.org/research/publications/libpb-2560].

Declarations

Ethics declaration not applicable.

Consent to publish declaration: not applicable.

Consent to participate declaration: not applicable.

Competing interests The authors declare no competing interests.

Open Access This article is licensed under a Creative Commons Attribution-NonCommercial-NoDerivatives 4.0 International License, which permits any non-commercial use, sharing, distribution and reproduction in any medium or format, as long as you give appropriate credit to the original author(s) and the source, provide a link to the Creative Commons licence, and indicate if you modified the licensed material. You do not have permission under this licence to share adapted material derived from this article or parts of it. The images or other third party material in this article are included in the article's Creative Commons licence, unless indicated otherwise in a credit line to the material. If material is not included in the article's Creative Commons licence and your intended use is not permitted by statutory regulation or exceeds the permitted use, you will need to obtain permission directly from the copyright holder. To view a copy of this licence, visit http://creativecommons.org/licenses/by-nc-nd/4.0/.

References

Adams IR, Davies OR (2023) Meiotic chromosome structure, the synaptonemal complex, and infertility. Annu Rev Genomics Hum Genet 24:35–61. https://doi.org/10.1146/annurev-genom-110122-090239

Anderson L, Royer S, Page S et al (2005) Juxtaposition of C(2)M and the transverse filament protein C(3)G within the central region of drosophila synaptonemal complex. Proc Natl Acad Sci U S A 102(12):4482–4487. https://doi.org/10.1073/PNAS.0500172102

Bilgir C, Dombecki CR, Chen PF et al (2013) Assembly of the synaptonemal complex is a highly temperature-sensitive process that is supported by PGL-1 during *Caenorhabditis elegans* meiosis. G3 Genes|Genomes|Genetics 3:585–595. https://doi.org/10.1534/g3.112.005165

Billmyre KK, Cahoon CK, Heenan GM et al (2019) *X* chromosome and autosomal recombination are differentially sensitive to disruptions in SC maintenance. Proc Natl Acad Sci U S A 116:21641–21650. https://doi.org/10.1073/pnas.1910840116

Billmyre KK, Kesler EA, Tsuchiya D et al (2023) SYCP1 head-to-head assembly is required for chromosome synapsis in mouse meiosis. Sci Adv 9:eadi1562. https://doi.org/10.1126/sciadv.adi1562

Blum M, Andreeva A, Florentino LC et al (2025) InterPro: the protein sequence classification resource in 2025. Nucleic Acids Res 53:D444–D456. https://doi.org/10.1093/nar/gkae1082

Brand CL, Cattani MV, Kingan SB et al (2018) Molecular evolution at a meiosis gene mediates species differences in the rate and patterning of recombination. Curr Biol 28:1289-1295e4. https://doi.org/10.1016/j.cub.2018.02.056

Cahoon CK, Yu Z, Wang Y et al (2017) Superresolution expansion microscopy reveals the three-dimensional organization of the drosophila synaptonemal complex. Proc Natl Acad Sci U S A 114:E6857–E6866. https://doi.org/10.1073/pnas.1705623114

Capilla-Pérez L, Durand S, Hurel A et al (2021) The synaptonemal complex imposes crossover interference and heterochiasmy in *Arabidopsis*. Proc Natl Acad Sci U S A 118:e2023613118. https://doi.org/10.1073/pnas.2023613118

Carpenter ATC (1975) Electron microscopy of meiosis in *drosophila melanogaster* females: I. Structure, arrangement, and temporal change of the synaptonemal complex in wild-type. Chromosoma 51:157–182. https://doi.org/10.1007/BF00319833

Carpenter A (1984) Recombination nodules and the mechanism of crossing-over in drosophila. Symp Soc Exp Biol 38:233–243

Collins KA, Unruh JR, Slaughter BD et al (2014) Corolla is a novel protein that contributes to the architecture of the synaptonemal complex of *Drosophila*. Genetics 198:219–228. https://doi.org/10.1534/genetics.114.165290

Feijão T, Marques B, Silva RD et al (2022) Polycomb group (PcG) proteins prevent the assembly of abnormal synaptonemal complex structures during meiosis. Proc Natl Acad Sci U S A 119:e2204701119. https://doi.org/10.1073/pnas.2204701119

Fernandes JB, Naish M, Lian Q et al (2024) Structural variation and DNA methylation shape the centromere-proximal meiotic crossover landscape in Arabidopsis. Genome Biol 25:30. https://doi.org/10.1186/s13059-024-03163-4

France MG, Enderle J, Röhrig S et al (2021) ZYP1 is required for obligate cross-over formation and cross-over interference in *Arabidopsis*. Proc Natl Acad Sci 118:e2021671118. https://doi.org/10.1073/pnas.2021671118

Gabler F, Nam S, Till S et al (2020) Protein sequence analysis using the MPI bioinformatics toolkit. Curr Protoc Bioinformatics 72:e108. https://doi.org/10.1002/cpbi.108

Girard C, Zwicker D, Mercier R (2023) The regulation of meiotic crossover distribution: a coarse solution to a century-old mystery? Biochem Soc Trans 51:1179–1190. https://doi.org/10.1042/BST20221329

Hartmann MA, Sekelsky J (2017) The absence of crossovers on chromosome *4* in *Drosophila melanogaster*: imperfection or interesting exception? Fly 11:253–259. https://doi.org/10.1080/19336934.2017.1321181

Hassold T, Hall H, Hunt P (2007) The origin of human aneuploidy: where we have been, where we are going. Hum Mol Genet 16:R203–R208. https://doi.org/10.1093/hmg/ddm243

Hawley RS, Irick H, Haddox DA et al (1992) There are two mechanisms of achiasmate segregation in *Drosophila* females, one of which requires heterochromatic homology. Dev Genet 13:440–467. https://doi.org/10.1002/dvg.1020130608

Hawley RS, Price A, Li H et al (2025) Patterns of crossover distribution in *drosophila mauritiana* necessitate a re-thinking of the centromere effect on crossing over. Genetics iyaf039. https://doi.org/10.1093/genetics/iyaf039

Higgins JD, Perry RM, Barakate A et al (2012) Spatiotemporal asymmetry of the meiotic program underlies the predominantly distal distribution of meiotic crossovers in barley. Plant Cell 24:4096–4109. https://doi.org/10.1105/tpc.112.102483

Hughes SE, Hawley RS (2020) Alternative synaptonemal complex structures: too much of a good thing? Trends Genet 36:833–844. https://doi.org/10.1016/j.tig.2020.07.007

Hughes SE, Miller DE, Miller AL, Hawley RS (2018) Female meiosis: synapsis, recombination, and segregation in *Drosophila melanogaster*. Genetics 208:875–908. https://doi.org/10.1534/genetics.117.300081

Hughes SE, Hemenway E, Guo F et al (2019) The E3 ubiquitin ligase Sina regulates the assembly and disassembly of the synaptonemal complex in drosophila females. PLoS Genet 15:e1008161. https://doi.org/10.1371/journal.pgen.1008161

Hughes SE, Staber C, McKown G et al (2025) The *Drosophilamauritiana* synaptonemal complex protein C(3)G repatterns the recombination landscape of *Drosophilamelanogaster*. PLoS Genet 21:e1011882. https://doi.org/10.1371/journal.pgen.1011882

Jang JK, Sherizen DE, Bhagat R et al (2003) Relationship of DNA double-strand breaks to synapsis in *Drosophila*. J Cell Sci 116:3069–3077. https://doi.org/10.1242/jcs.00614

Jeffress JK, Page SL, Royer SM et al (2007) The formation of the central element of the synaptonemal complex may occur by multiple mechanisms: the roles of the N- and C-terminal domains of the drosophila C(3)G protein in mediating synapsis and recombination. Genetics 177:2445–2456. https://doi.org/10.1534/genetics.107.078717

Jeon S, Jeon Y, Lim J-Y et al (2025) Emerging regulatory mechanisms and functions of biomolecular condensates: implications for therapeutic targets. Signal Transduct Target Ther 10:4. https://doi.org/10.1038/s41392-024-02070-1

Joyce EF, McKim KS (2010) Chromosome axis defects induce a Checkpoint-Mediated delay and interchromosomal effect on crossing over during drosophila meiosis. PLoS Genet 6:e1001059. https://doi.org/10.1371/journal.pgen.1001059

Koehler KE, Hawley RS, Sherman S, Hassold T (1996) Recombination and nondisjunction in humans and flies. Hum Mol Genet 5:1495–1504. https://doi.org/10.1093/hmg/5.Supplement_1.1495

Köhler S, Wojcik M, Xu K, Dernburg AF (2025) Dynamic molecular architecture of the synaptonemal complex. Sci Adv. https://doi.org/10.1126/sciadv.adq9374

Kondo S, Ueda R (2013) Highly improved gene targeting by germline-specific Cas9 expression in *Drosophila*. Genetics 195:715–721. https://doi.org/10.1534/genetics.113.156737

Kumar M, Michael S, Alvarado-Valverde J et al (2024) ELM—the eukaryotic linear motif resource—2024 update. Nucleic Acids Res 52:D442–D455. https://doi.org/10.1093/nar/gkad1058

Kursel LE, Cope HD, Rog O (2021) Unconventional conservation reveals structure-function relationships in the synaptonemal complex. elife 10:e72061. https://doi.org/10.7554/eLife.72061

Kursel LE, Martinez JEA, Rog O (2023) A suppressor screen *in C. elegans* identifies a multiprotein interaction that stabilizes the synaptonemal complex. Proc Natl Acad Sci U S A 120:e2314335120. https://doi.org/10.1073/pnas.2314335120

Lake CM, Nielsen RJ, Guo F et al (2015) Vilya, a component of the recombination nodule, is required for meiotic double-strand break formation in drosophila. elife 4:e08287. https://doi.org/10.7554/eLife.08287

Lake CM, Gardner J, Briggs S et al (2024) The deubiquitinase Usp7 in *Drosophila melanogaster* is required for synaptonemal complex maintenance. Proc Natl Acad Sci 121:e2409346121. https://doi.org/10.1073/pnas.2409346121

Lantz V, Chang JS, Horabin JI, Bopp D, Schedl P (1994) The Drosophila orb RNA-binding protein is required for the formation of the egg chamber and establishment of polarity. Genes Dev 8(5):598–613

Libuda DE, Uzawa S, Meyer BJ, Villeneuve AM (2013) Meiotic chromosome structures constrain and respond to designation of crossover sites. Nature 502:703–706. https://doi.org/10.1038/nature12577

Llano E, Pendás AM (2023) Synaptonemal complex in human biology and disease. Cells 12:1718. https://doi.org/10.3390/cells12131718

Lloyd A, Morgan C, Franklin H, Bomblies FC K (2018) Plasticity of meiotic recombination rates in response to temperature in *Arabidopsis*. Genetics 208:1409–1420. https://doi.org/10.1534/genetics.117.300588

Ludwiczak J, Winski A, Szczepaniak K et al (2019) Deepcoil—a fast and accurate prediction of coiled-coil domains in protein sequences. Bioinformatics 35:2790–2795. https://doi.org/10.1093/bioinformatics/bty1062

Lupas A, Van Dyke M, Stock J (1991) Predicting coiled coils from protein sequences. Science 252:1162–1164. https://doi.org/10.1126/science.252.5009.1162

Martins T, Maia AF, Steffensen S, Sunkel CE (2009) Sgt1, a co-chaperone of Hsp90 stabilizes Polo and is required for centrosome

organization. EMBO J 28:234–247. https://doi.org/10.1038/emboj.2008.283
McKim KS, Dahmus JB, Hawley RS (1996) Cloning of the *drosophila melanogaster* meiotic recombination gene mei-218: a genetic and molecular analysis of interval 15E. Genetics 144:215–228. https://doi.org/10.1093/genetics/144.1.215
McLachlan AD, Stewart M (1975) Tropomyosin coiled-coil interactions: evidence for an unstaggered structure. J Mol Biol 98:293–304. https://doi.org/10.1016/S0022-2836(75)80119-7
Mehrotra S, McKim KS (2005) Temporal analysis of meiotic DNA double strand break formation and repair in drosophila females. PLoS Genet Preprint e200. https://doi.org/10.1371/journal.pgen.0020200.eor
Miller DE, Smith CB, Kazemi NY et al (2016) Whole-genome analysis of individual meiotic events in *Drosophila melanogaster* reveals that noncrossover gene conversions are insensitive to interference and the centromere effect. Genetics 203:159–171. https://doi.org/10.1534/genetics.115.186486
Morgan C, Fozard JA, Hartley M et al (2021) Diffusion-mediated HEI10 coarsening can explain meiotic crossover positioning in *Arabidopsis*. Nat Commun 12:4674. https://doi.org/10.1038/s41467-021-24827-w
Neves ARR, Čavka I, Rausch T, Köhler S (2025) Crossovers are regulated by a conserved and disordered synaptonemal complex domain. Nucleic Acids Res 53:gkaf095. https://doi.org/10.1093/nar/gkaf095
Page SL, Hawley RS (2001) *c(3)G* encodes a *Drosophila* synaptonemal complex protein. Genes Dev 15:3130–3143. https://doi.org/10.1101/gad.935001
Page S, Nielsen RJ, Teeter K et al (2007) A germline clone screen for meiotic mutants in *Drosophila melanogaster*. Fly 1:172–181. https://doi.org/10.4161/fly.4720
Page SL, Khetani RS, Lake CM et al (2008) Corona is required for higher-order assembly of transverse filaments into full-length synaptonemal complex in drosophila oocytes. PLoS Genet 4:e1000194. https://doi.org/10.1371/journal.pgen.1000194
Parry DAD (1982) Coiled-coils in α-helix-containing proteins: analysis of the residue types within the heptad repeat and the use of these data in the prediction of coiled-coils in other proteins. Biosci Rep 2:1017–1024. https://doi.org/10.1007/BF01122170
Pazhayam NM, Turcotte CA, Sekelsky J (2021) Meiotic crossover patterning. Front Cell Dev Biol 9:681123. https://doi.org/10.3389/fcell.2021.681123
Pazhayam NM, Sagar S, Sekelsky J (2025) Suppression of meiotic crossovers in pericentromeric heterochromatin requires synaptonemal complex and meiotic recombination factors in *drosophila melanogaster*. Genetics 229:iyaf029. https://doi.org/10.1093/genetics/iyaf029
Plough HH (1917) The effect of temperature on crossingover in *drosophila*. J Exp Zool 24:147–209. https://doi.org/10.1002/jez.1400240202
Rog O, Köhler S, Dernburg AF (2017) The synaptonemal complex has liquid crystalline properties and spatially regulates meiotic recombination factors. elife 6:e21455. https://doi.org/10.7554/eLife.21455
Rogakou EP, Pilch DR, Orr AH et al (1998) DNA double-stranded breaks induce histone H2AX phosphorylation on serine 139. J Biol Chem 273:5858–5868. https://doi.org/10.1074/jbc.273.10.5858
Scott Hawley R, Theurkauf WE (1993) Requiem for distributive segregation: achiasmate segregation in drosophila females. Trends Genet 9:310–316. https://doi.org/10.1016/0168-9525(93)90249-H
Sekelsky J (2017) DNA repair in *Drosophila*: mutagens, models, and missing genes. Genetics 205:471–490. https://doi.org/10.1534/genetics.116.186759
Sen S, Dodamani A, Nambiar M (2023) Emerging mechanisms and roles of meiotic crossover repression at centromeres. In: Cole F (ed) Current topics in developmental biology. Elsevier, pp 155–190
Takeo S, Lake CM, Morais-de-Sá E et al (2011) Synaptonemal complex-dependent centromeric clustering and the initiation of synapsis in drosophila oocytes. Curr Biol 21:1845–1851. https://doi.org/10.1016/j.cub.2011.09.044
True JR, Mercer JM, Laurie CC (1996) Differences in crossover frequency and distribution among three sibling species of *drosophila*. Genetics 142:507–523. https://doi.org/10.1093/genetics/142.2.507
Voelkel-Meiman K, Cheng S-Y, Morehouse SJ, MacQueen AJ (2016) Synaptonemal complex proteins of budding yeast define reciprocal roles in MutSγ-mediated crossover formation. Genetics 203:1091–1103. https://doi.org/10.1534/genetics.115.182923
Von Diezmann L, Bristow C, Rog O (2024) Diffusion within the synaptonemal complex can account for signal transduction along meiotic chromosomes. Mol Biol Cell 35:ar148. https://doi.org/10.1091/mbc.E24-05-0225
Wang K, Wang C, Liu Q et al (2015a) Increasing the genetic recombination frequency by partial loss of function of the synaptonemal complex in rice. Mol Plant 8:1295–1298. https://doi.org/10.1016/j.molp.2015.04.011
Wang S, Zickler D, Kleckner N, Zhang L (2015b) Meiotic crossover patterns: obligatory crossover, interference and homeostasis in a single process. Cell Cycle 14:305–314. https://doi.org/10.4161/15384101.2014.991185
Williams S, Hawley RS (2025) From conservation to adaptation: understanding the synaptonemal complex's evolutionary dynamics. Curr Opin Genet Dev 93:102349. https://doi.org/10.1016/j.gde.2025.102349
Zakian VA (2012) Telomeres: the beginnings and ends of eukaryotic chromosomes. Exp Cell Res 318:1456–1460. https://doi.org/10.1016/j.yexcr.2012.02.015
Zhang Z, Xie S, Wang R et al (2020) Multivalent weak interactions between assembly units drive synaptonemal complex formation. J Cell Biol 219:null. https://doi.org/10.1083/jcb.201910086
Zhang L, Stauffer W, Liu C et al (2025) Crossover patterning through condensation and coarsening of pro-crossover factors. Nat Cell Biol 27:1161–1174. https://doi.org/10.1038/s41556-025-01688-9
Zimmermann L, Stephens A, Nam S-Z et al (2018) A completely reimplemented MPI bioinformatics toolkit with a new HHpred server at its core. J Mol Biol 430:2237–2243. https://doi.org/10.1016/j.jmb.2017.12.007
Zitron AE, Hawley RS (1989) The genetic analysis of distributive segregation in *drosophila melanogaster*. I. Isolation and characterization of aberrant X segregation (Axs), a mutation defective in chromosome partner choice. Genetics 122:801–821. https://doi.org/10.1093/genetics/122.4.801

Publisher's Note Springer Nature remains neutral with regard to jurisdictional claims in published maps and institutional affiliations.